A fluorescence microscopy image showing numerous melanoma cells. The cells are stained with a green fluorescent dye, highlighting their nuclei and cytoplasm. The cells exhibit a variety of shapes and sizes, some with prominent nuclei and others with more diffuse staining. The background is dark, making the green-stained cells stand out.

IMPEDANCE-BASED BIOASSAY FOR CHARACTERIZATION OF SINGLE MALIGNANT MELANOMA CANCER CELLS USING CMOS- MEA SYSTEMS

A HETEROGENEITY AND CLASSIFICATION ASSAY PROPOSAL

MAKRINA SEKERI (4515668)

Delft, 2018

IMPEDANCE-BASED BIOASSAY FOR CHARACTERIZATION OF SINGLE MALIGNANT MELANOMA CANCER CELLS USING CMOS-MEA SYSTEMS

A HETEROGENEITY AND CLASSIFICATION ASSAY PROPOSAL

by

Makrina Sekeri

In partial fulfillment of the requirements for the degree of

Master of Science
In Biomedical Engineering

at the Delft University of Technology,

to be defended publicly on Monday July 16, 2018 at 14:00 AM.



TU Delft supervisors: prof.dr.ir. R. Hendriks
prof.dr.ir. V. Valente

imec supervisors: CTT, dr. D. Braeken

TU Delft supervisors:	Prof.dr.ir. W. Serdijn,	TU Delft
	Prof. dr. ir. V. Valente,	TU Delft
	prof.dr.ir. R. Hendriks,	TU Delft
	CTT, dr. D. Braeken,	IMEC

Keywords: *Malignant Melanoma, MM, cancer, impedance, bioassay, multielectrode array, MEA, HD-MEA, adhesion, drug resistance, classification, heterogeneity, single-cell*

Copyright©2018 by M. Sekeri

An electronic version of this dissertation will be available at: <http://repository.tudelft.nl>

*To my family and friends; my mentors in life.
To all those who are a living inspiration in this world, and don't even know it;
to our everyday heroes.*

ABSTRACT

Malignant Melanoma (MM) is the most aggressive type of skin-cancer. Current diagnostic tools for the detection of malignancies of the skin (MM cancer) include histological, optical, ultrasound, and impedance-based techniques. The inadequacies of the first three practices are overwhelmed by the Electrical Impedance Spectroscopy (EIS) method. EIS overcomes reported spatiotemporal tradeoffs as a label-free and optics-free analytical method. Yet, MM's enhanced heterogeneity and metastatic potential still results in misdiagnosis, or late diagnosis leading to stages characterized by high mortality rates. Important biological information and processing ability on single-cell level is missing. Single-cell dynamics recorded with a high-throughput system, contain important biological information on the heterogeneous subpopulations which are responsible for the MM aggressiveness.

This project aims to investigate experimentally the possibility and capabilities of such a bioassay development, create working protocols and generate a fundamental basis for analysis and interpretation of the big-data-sets which derive from Impedance monitoring from a high-throughput transducer.

Experiments were performed, employing two diverse, human-derived, MM cancer cell-lines, and using a high-throughput HD-MEA system with a 1024-channel impedance readout unit developed at IMEC, in Belgium. The measurements were realized at 1kHz aiming to extract R_{seal} information. The main proposal presents an experimental protocol of mid-term and long-term experiments Temporal and spatial resolutions were enhanced (Control System Automation), allowing for implementation of an experimental set to test the assay's capabilities and determine any necessary additions to make the assay more robust for research (i.e. Z-Map, templates and scripts for OriginLab and Matlab, statistical methods for validation of findings on the big-data sets, optimizations in the experimental process, etc).

Experimental results proved the optics-free specification of the assay with the utilization of an Impedance colormap, which was validated by comparing it to confocal images after measurements. Electrode-size and normalization techniques were deemed crucial factors that affected the variance of the results for the largest and smallest electrode sizes. Confluence level (70% or 10%) of the cell on the chip was an added biasing factor. IM measurements at 1kHz for two MM cell-lines (MM087 & MM029) showed a good possibility for classification (long-term experiments), while the biological findings on the heterogeneity information (mid-term and long-term experiments) cannot be considered conclusive until a full-scale analysis is conducted on the data. A proposal for a new type of analysis on the Impedance data is presented; it is an example-based approach to extract the classification and heterogeneity information of normalized IM measurements, by obtaining and analyzing the trends of impedance variance over time, per electrode.

The bioassay proposal that was developed and tested in this project shows potential for both classification and heterogeneity studies for MM cancer. Further experimentation and development of validation techniques is required.

Acknowledgements

With the completion of this project there are a number of people I owe my gratitude and would like to thank.

My TU Delft supervisors for always being there to guide and support me from afar, until the completion of this project. Richard and Vivo, I honestly appreciated and loved working with the both of you, through the good and the challenging moments we shared. You were a rock to me. Thank you!

My imec supervisors, Dries and Carl, for providing me with the opportunity to join them in IMEC and allowed me to explore many of my ideas in research. You made me part of the CTT group which I will always remember so fondly! In this dynamic and challenging environment, you always believed that I could make it even when things looked really down.

I would also like to thank the members of the committee (Wouter and my supervisors) for taking time during the holidays to group up and participate as members in my defense.

Everyone that lent their expertise during this project: Olga, Bastien, Bea, Erku, Luo, Thomas, Niels, and all the rest of the CTT group, thank you. Jan, for sharing your expert opinion with Labview, and my desk-buddy for joining me in my brainstorming that long-day, I really appreciate it!

Vale and Vag, who always believed in me during this Master's program, even from afar. My friends from the Netherlands and Belgium, for sharing all those great – and sometimes crazy – moments together that made this long ride a good one. I am sorry I cannot write all your names here.

Gokul, thank you for all the talks, the laughter and the time we shared since Project MARCH. During rather stressful times of this project, you were always there, supporting me with a smile and care.

Luci and Kosta, I am really happy I got to meet you and create this great friendship from inside our program! Thank you for always making me smile and being there to overcome together the challenges of the past 3 years. We did it! :) I will miss for now the carbonara nights with you and Jacy, but I know that these were only a beginning to the ones to come.

Christinaki, my unbiological sister and partner in crime, thank you for always being there, without even needing to be there! You helped me a lot during so many tough times during this project (and not only), but at the same time you also shared my utmost joys! Thanks for everything.

Mum and Dad, you made this dream feasible. Thank you and Peter, from the bottom of my heart for always supporting me and being there no matter what! I am very grateful to have you in my life. You made all of this possible and I cannot begin to express how much you mean to me; This degree, is for you.

CONTENTS

Abstract

Acknowledgements

1. Introduction & Literature

1.1. Biological Background

1.1.1. Cancer and Tumor-Heterogeneity

- Cancer Initiation
- Metastasis and Tumor-Heterogeneity

1.1.2. Malignant Melanoma (MM) Cancer

1.2. Melanoma Diagnosis

- In-vitro Cell Cultures

1.3. Problem Statement

1.4. Thesis Structure

2. Impedance Spectroscopy for Cell-Analysis

2.1. Impedance

2.2. Fundamentals of Electrical Impedance Spectroscopy in Cancer

2.3. Equivalent Circuits and the Cell-Electrode Interface

2.3.1. Equivalent Circuit: Electrode-Electrolyte Interface Model

2.3.2. Equivalent Circuit: Tissue Model

2.3.3. Equivalent Circuit: Single-Cell on-Chip Model

2.4. Multi-Electrode Array Systems for Single-cell Assays & Analysis

2.4.1. An Introduction to MEA Systems

2.4.2. Plating cells on MEA transducers for experimentation

2.4.3. MEA Modalities and Data Acquisition-and-Processing

3. Impedance-based Bioassay

3.1. Methods & Systems

3.1.1. Cell-Cultures: Malignant Melanoma Cell-Lines

3.1.2. MEA Platforms: Prototype HD CMOS-MEA System

- Specifications: IM and EIS Modalities
- Control-system Design: IM and EIS Automations

3.1.3. MEA Platforms: Passive HD MEA (Commercial System)

3.2. The Bioassay

3.2.1. Experimental-process: Considerations

3.2.2. Experimental-process: Methods

- [Reference Electrodes and Sterility](#)
- [Data Processing, Analysis, and Validation](#)
- [MEA Layout Considerations](#)
- [Confocal Microscopy & Impedance Map for optic-free Assay Validation](#)
- [Chip Preparation for Cell-experiments](#)

3.2.3. Proposed Experimental Protocol

4. Experimental Process

4.1. Experimental Report: Findings

4.1.1. Impedance-based cell response for diverse electrode sizes @ 1kHz

4.1.2. EIS Information The spectrum response

4.2. Over-Time IM Measurements: Realizing the Bioassay

4.2.1. Experimental Reporting

- [Log 1](#)
- [Main Findings](#)
- [Discussion 1A: Classification of MM cell-lines](#)
- [Discussion 2A: Heterogeneity of MM cell-lines](#)
- [Discussion 1B: Heterogeneity of MM cell-lines](#)
- [Log 2](#)
- [Main Findings](#)

4.2.2. Impedance-Colormap in replacing Confocal Images

4.2.3. A future analysis-tool to extract classification and heterogeneity information from the impedance data

4.3. Summary & Conclusions

5. Discussion & Prospects

5.1. Discussion

- [Precursor Drug-Testing experiments with the Bioassay](#)

5.2. Prospects

[List of Abbreviations](#)

[Appendix](#)

[References](#)

1.

Introduction & Literature

*"The greater our knowledge increases, the more our
ignorance unfolds."*

J.F. Kennedy

In this chapter, biological background is given on cancer, metastatic process, and intratumoral-heterogeneity. The Malignant Melanoma (MM) form of cancer is introduced as a promising biological model for unlocking crucial information in cancer progression (heterogeneous-linked metastatic potential and drug-resistance). Currently used diagnostic tools for MM are presented. Impedance Spectroscopy is endorsed as a method for MM diagnosis addressing various of the inadequacies of the other diagnostic methods. However, important biological information on single-cell level is still missing, leading to misdiagnosis, metastatic behavior, and treatment-resistance. These insufficiencies of current diagnostics reveal necessity for a label-free bioassay development to be used in cell-lines' classification and in the extraction of vital biological information of distinct cell-subpopulations. A need towards "true" single-cell platforms for in-vitro cancer progression studies and diagnosis is stressed. Commonly used interfaces for experimentation in-vitro, introduce high-Density Multielectrode Array (MEA) systems, which only recently achieved high-throughput specifications. Based on these grounds, this project's research question is formed, aiming to combine the previously discussed systems and theories, to develop a novel single-cell, impedance-based bioassay for MM research and diagnosis.

1.1 Biological Background

1.1.1 Cancer and Tumor-Heterogeneity

Cancer Initiation

According to the National Cancer Institute (NCI), *cancer* is a generic term used to describe diseases that implicate uncontrollable and abnormal cell-division, with a tendency towards invasion and colonization to other tissues [1]. When cancer is initiated, a process known as *tumorigenesis*, normal (healthy) cells suffer multiple mutations and they eventually transform into malignancies.

Various centers have been trying to identify the source of the mutations that lead to cancer. The International Agency for Research on Cancer (IARC) – employed by the World Health Organization (WHO) – has classified cancer-causality as a combination of genetic predisposition and environmental exposure to carcinogenic agents which affect the *epigenetics*¹ of the cell (i.e. tumor microenvironment): physical, chemical and biological. For instance, Ultra-Violet (UV) radiation, food or water contaminants (like aflatoxin and arsenic respectively), tobacco components, and certain viral or bacterial infections [2]. Age is another factor that has been salient to influence transformation of cells to malignant as the cellular repair-mechanisms tend to degenerate with time; this allows mutations to occur and dominate more often. However, cancer initiation is only part of the disease's pathogenesis, since its progression is the major clinical concern.

Metastasis and Tumor-Heterogeneity

The tendency of tumor cells to invade other tissues, is called *metastasis*, an imminent threat to all cancer-patients, as it is responsible for approximately 90% of cancer-induced deaths. Lee et al. notably defined metastasis as a complex process, very dynamic, which can be effectively characterized as a multistep, secondary-tumor formation [3], [4]. This inclination of tumor cells defines the *progression of cancer*, otherwise called *metastatic potential*.

The metastatic process involves a cascade of steps (see Figure 1). Initially, some tumor-cells *detach*² from the substrate and from each other, due to changes in their adhesive molecular structure (i.e. lytic enzymes release). Next, they enter the blood stream that has been formed around them (Angiogenesis, Local Invasion and Intravasation processes) and they travel through the blood stream or lymph nodes around the patient's body. Hereafter, a subpopulation will gain a selective advantage over other tumor-cells that will die along their journey (Dissemination process of Circulating Tumor Cells, CTCs). These survivors are the ones to finally exit the bloodstream and colonize to the new sites (Extravasation and Colonization processes). This last step is realized by cell adhesion and initiation of proliferation.

¹ Epigenetics: Changes in the genetic characteristics of a cell (affecting morphology and functionality) due to external factors. Genetic mutations are by common ground irreversible, while epigenetic aberrations are occurring on a single-cell level within a tumor dynamically; they are a dominant factor in intratumoral heterogeneity [5].

² Some of the cancerous-mutations cripple the cell's apoptotic mechanisms (i.e. self-induced death) that would have otherwise initiated at the moment of detachment-detection from the Extracellular Matrix (ECM). Involved proteins, molecules and receptors: Integrins and Cadherins, Selectins, CD44 Members, Immunoglobulin Superfamily (IgSF).

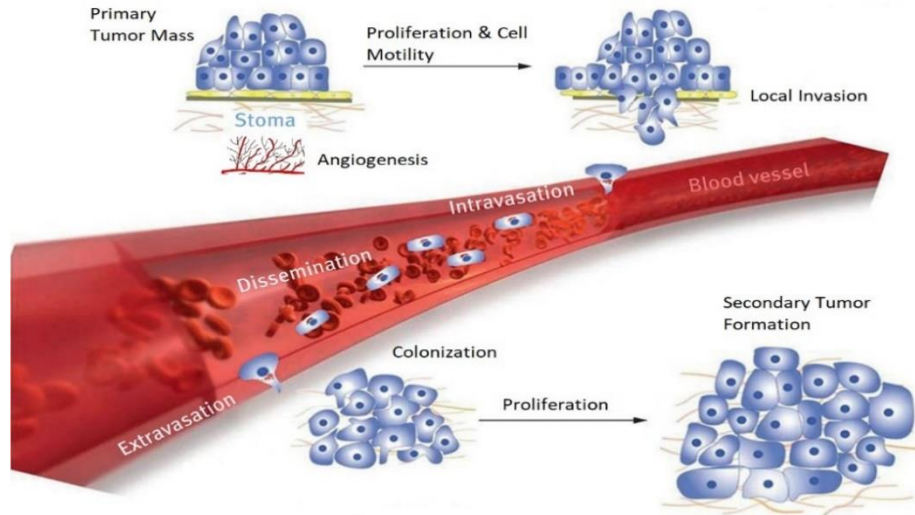


Figure 1. The Metastatic Cascade [6].

The newly formed tumor is usually more aggressive (i.e. enhanced metastatic potential) and resistant to treatment compared to the initial mass. This distinct behavior has been largely attributed to the aberrant epigenetic mutations that occur over time in the tumor microenvironment. These are known to generate subpopulations of cells with disparate characteristics, as well as the selective advantage, to both initiate and survive the metastatic cascade, settling into the distant tissue. The existence of these sub-populations reveals a within-tumoral heterogeneity, i.e. *intra-tumoral heterogeneity*.

Heterogeneity can be observed both between and within tumors. Understanding the full spectrum of mutations which lead to heterogeneous cell-populations has been useful for unlocking both causality and intrinsic characteristics of disease progression. Intra-tumor variation is likely to result in rigorous tumor-adaptation to microenvironmental transitions, such as drug-introduced changes. Hence, the clinical implications are many, with dynamic adaptation leading often to therapy-resistance and histological variation, reducing the validity of a partial biopsy [7]. The next two paragraphs explain how this takes effect.

There are two main theories used to explain and justify tumorigenesis with heterogenous properties: the *clonal evolution theory* and the *Cancer Stem-Cell (CSC) theory*. The former introduces the concept of accumulative somatic mutations as the cause for cancer development, following Darwin's selection-model, i.e. the "survival of the fittest". In this model all surviving cells have equal potential for inducing tumorigenesis, and this has indeed been noticed for certain cases. However, it does not explain most cancers' evolution-characteristics towards malignancy. In the second theory, it is hypothesized that the main reason for cancer heterogeneity falls on a specific subpopulation of the tumor-mass that expresses stem-cell³-like properties and phenotypic characteristics: the multipotent Cancer Stem Cells (CSCs). These CSCs have been identified in various cancers (like brain, blood, lung, prostate, skin-melanomas, breast, etc) and recently was reported that they are to blame for enhanced tumorigenic capacity and malignancy [8].

³ Stem Cells: Cells with the capability of differentiating (i.e. develop phenotype and characteristics of a certain tissue cell). There are two types of stem-cells: *Pluripotent* and *Multipotent*. The former are embryonic cells that may differentiate to any cell-type of the body, while the latter can develop to more than one cell-type but not to all.

While every cell in the population is genetically equal, the previously-mentioned subpopulations exhibit the ability of asymmetric cellular division. Such properties lead to the creation of two main sub-sets of cells: none or less-tumorigenic cells that influence the overall traits of existing tumors, and the self-renewal of the CSCs cells which will further differentiate into a cell-type in accordance with their genetic and epigenetic status. This dependency on the tumor microenvironment is called *cellular plasticity* and is an important aspect in cancer. As the daughter-cells acquire characteristics of the parent-cell including differentiation traits, cellular reprogramming may result in de-differentiation of the daughter-cell if the epigenetics change (i.e. drug delivery). This is what makes the heterogeneous process quite dynamic and thus it is considered to be the main contributor to cancer aggressiveness and poor prognosis, leading to (inevitable) disease relapses in many cases.

Having analyzed tumorigenesis (i.e. cancer initiation) and cancer aggressiveness (i.e. metastatic potential, therapy-resistance, and relapse danger) by considering the within-tumoral heterogeneity of a cancerous cell-population, the importance of studying and understanding the underlying processes involved became evident. The given theories, may explain some characteristics and functions of various cancer-types. Yet, rigorous study of suitable biological cancer-models with intense expression of the aforementioned characteristics is still deemed necessary using appropriate technological means. In the next sub-chapter, it will be seen that Malignant Melanoma is a great biological model to use, which is why it was chosen for the purpose of this project.

1.1.2 Malignant Melanoma (MM) Cancer

According to WHO, by 2030, 346,157 people worldwide will obtain MM cancer; many will suffer the danger of misdiagnosis or late detection, leading to casualties of about 86,006 patients due to metastasis and deeply-penetrated melanomas [2]. *Malignant Melanoma (MM)* is the most aggressive type of skin-cancer. It is caused from a series of mutations occurring in the *melanocytes*, cells which are mostly found in the interface between the epidermis and dermis layers, as well as in the basal layer of the epidermis (Figure 2).

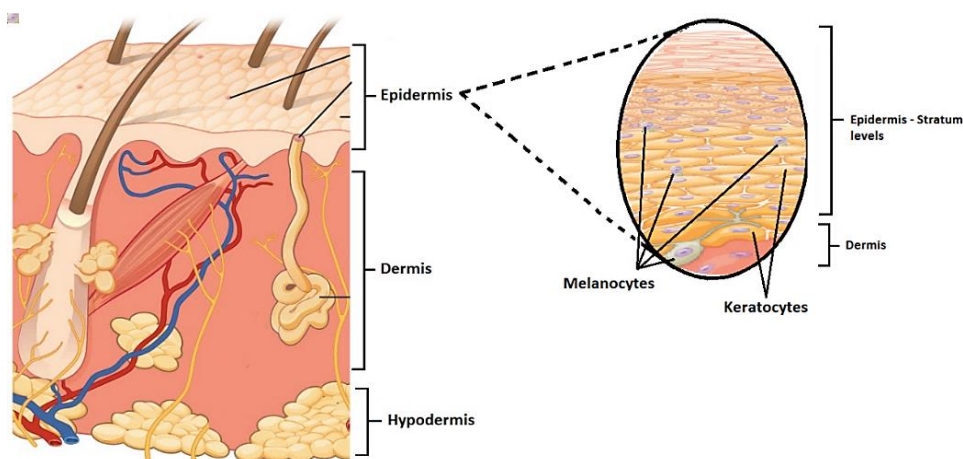


Figure 2. Skin Layers and Melanocyte cells.

This figure is a combination of two pictures found in this domain: [9]. Only the necessary information is depicted.

Melanocytes are anchored via dendritic-formation to their prominent neighboring-epidermal-cells (i.e. the keratocytes) and their main function is to produce a pigment called *melanin*. Melanin gives hair and skin their color, while it protects the epidermis cells by absorbing the harmful UV radiation [10]. However, this radiation may eventually damage and mutate these cells and in time lead to MM cancer. The affected areas are then renamed to *melanomas* (i.e. *melanoma cells*). Based on histological observation, five main stages of MM cancer are recognized (0 to IV): (i) benign nevi, (ii) dysplastic nevi, (iii) radial-growth phase (RGP), (iv) vertical-growth phase (VGP), and (v) metastatic melanoma. Figure 3 illustrates the differences between the progression during the different stages.

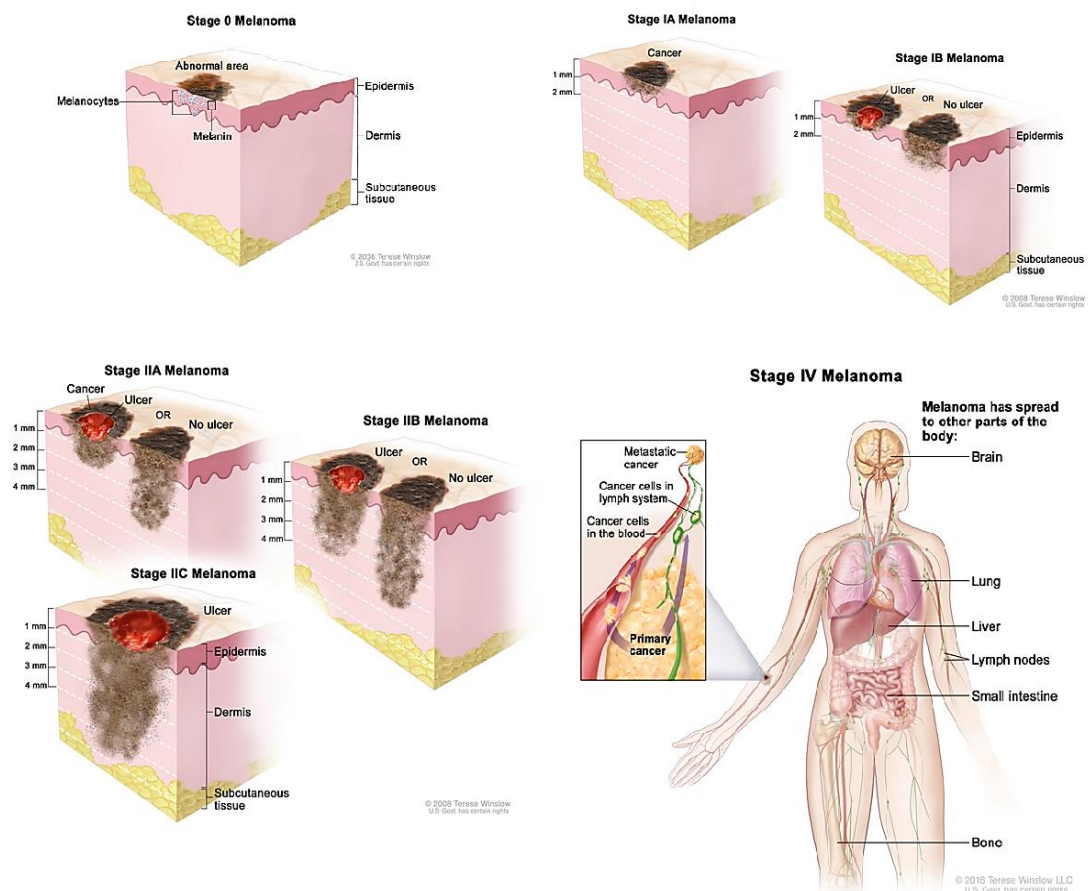


Figure 3. The five stages of Malignant Melanoma [1].

If identified at an early stage, melanomas can be treated effectively. However, for a large portion of MM patients this is not the case. The main reason lies in the increased heterogeneous signature of the MM cells, which was proved to include minorities of cancerous cells with stem-cell plasticity. In this case, there is strong correlation between MM progression (i.e. metastatic aggressiveness and drug resistance) and single-cell microenvironment properties, making MM an interesting case for research.

1.2 Melanoma Diagnosis

In 2010, S.S. Ringel et al. reviewed 25 years in Melanoma Diagnostics. Until the 1980s, melanoma was recognized only at advanced stages, when the pigmented lesion was fairly large or bleeding (i.e. ulcerated). Around 1985, full-body screenings and mnemonics⁴ were introduced and verified by the medical community as a good practice [4]. Since the 1990s, golden standards in melanoma diagnostics have been the dermoscopy and histopathology examinations. Both are performed by a specialist physician.

Histological diagnostics involve biopsying the lesion and identifying whether the lesion is benign or malignant with confocal microscopy. False negatives often occur since the increased mutagenic expression of cancer cells may result in certain protein-markers' loss [11]. Histological examinations lose their validity for highly heterogeneous cancers, since the results depend on the obtained sample, affecting its accuracy [23]. The majority of the dyes used are cell-toxic and prohibit long-term experimentation. Still, it is used a lot as a diagnostic tool as it performs tests with single-cell resolution and is well-known by clinicians.

Optical-based methods and **Ultrasound Waves**, provide a noninvasive means of diagnosis for MM cancer. A popular method used in principle for diagnostics is the Dermoscopy. Doctors obtain images with a camera system to compare over different examinations. The light-based visual technology of a dermoscope allows in vitro visualization of the inner skin layer down to the under epidermis and upper dermis regions. Even by achieving a highly increased resolution, it is failing to identify early atypical melanomas based mostly on the expertise of the attending doctor [4], [14]. Other optical-based tools have started to surface aiming to increase the specificity of the final diagnosis. Such devices are Optical Coherence Tomography (OCT) equipment, Interferometers, or High-frequency Ultrasound machines [4], [13], [12].

Despite the increased efficiency of these tools, misdiagnosis at an early stage is still the leading cause of MM cancer progression to untreatable stages. In addition, optical-based techniques have usually poor spatial resolution or low depth. Hence, effective treatment of MM requires more accurate disease classification bioassays, early diagnosis and further understanding of the underlying mechanisms of metastasis.

Table 1 lists the advantages and disadvantages of the presented diagnostic tools. Two or more of the methods are usually complemented to strengthen the reliability of current diagnostics. The main reason behind this lack of concrete diagnostics is reflected in the biology of MM itself, characterized by enhanced heterogeneity with stem-cell plasticity. As stated in previous sections, cell-adhesion and detachment from a small subset of cells were identified as key-steps in cancer initiation and progression. Often this distinct information is masked by measuring the average demeanor of a bulk portion from the cell-population on tissue level, or by performing histological tests with markers that overlap for different MM cell-lines. Those measurements are then called *ensembled* and they lose the efficiency of single-cell resolution. In addition, long-term experimentation is commonly prevented in histological examination (e.g. confocal dyes' toxicity), limiting the capacity of existing bioassays. These reasons constitute why MM is both a suitable biological model to study highly mutagenic cancer behavior, as well as why it is very difficult to have replicable specificity from *ensembled* measurements and the current tools.

⁴ Most famous mnemonic is the ABCD: "Asymmetry", "Border irregularity", "Color variegation", "Diameter>6mm".

Table 1. Malignant Melanoma Diagnostics: Pros and Cons.

<i>Diagnostic Techniques & Tools</i>	SYSTEM	ADEQUATE DEPTH	HIGH SPATIAL RESOLUTION	SINGLE-CELL RESOLUTION	LABEL-FREE Long-Term Experimentation feasibility
High-frequency Ultrasound (HUS)	Uses pressure sound waves and collects time-delay. Creates depth-resolved images.	X	✓	✓	✓
		Low-depth but high-spatial resolution is a challenge to discriminate benign from pigmented lesions in situ [12].			
Low-frequency Ultrasound (LUS)	Gives information mostly on the inflammation processes involved [4].	✓	X	✓	✓
		High-depth but low-spatial resolution is a challenge to provide statistically significant (i.e. concrete) diagnostic conclusions [12], while metastatic melanomas cannot be distinguished from other metastatic cancer cell-types [14].			
Optical Coherence Tomography (OCT, and other classes i.e. High Definition OCT, etc)	Uses interferometry ^a .	✓	X	N/A ^c	✓
		OCT has low depth-resolution to replace histology and classification of cell-lines is then not possible [12]. It also lacks information on the morphology of the cells [14]. Promising is the High Definition-OCT class which has high-depth resolution, but the limited field of view reduces significantly the spatial-resolution (still lacking to confocal imaging) [4], [12], [13].			
Dermoscopy	Uses Epiluminescence Microscopy or Dermoscopy ^b .	X	✓	X	✓
		Allows in-vivo visualization of the epidermis and papillary dermis that are normally missed with the naked eye. It masks heterogeneous single-cell behavior. Increases specificity in distinguishing a malignant from a benign lesion, but the effectiveness is biased by the expertise of the attending physician and the size of the diameter of the lesions [4], [14].			
Histology	Involves biopsying a sample and lab work involving confocal microscopy ^d .	N/A	N/A	✓	X
		Besides being highly invasive, histology examinations lose their validity for highly heterogeneous cancers, since the results will depend on the sample making it not always 100% accurate [23]. The majority of the dyes used are cell-toxic and prohibit long-term experimentation. Such are calcein AM, DAPI, phalloidin, etc.			
Total Body Tomography	PET and MRI scans [14].	N/A	N/A	✓	X
		<u>MRI</u> : Shows clear differentiation between healthy and cancerous cells of the dermis and epidermis. Is time consuming and requires expensive equipment and specialized place for installation. Patients with metal implants are prohibited from MRI examination. <u>PET</u> : Is less expensive than MRI and costlier than Ultrasound. It detects metabolic-activity variations to distinguish between malignant and benign lesions. Its sensitivity decreases for smaller tumor sizes.			

^a Splits a monochromatic light-source of constant phase – allows coherence – into two paths (i.e. *Reference Path* – terminates to a mirror; and *Sample Path* – where tissue absorbs or scatters it) and then when they are recombined, any difference in the lengths of the paths will cause them to interfere with each other. In near Infrared wavelengths scattering is the dominant effect.

^b Clinical term used for describing the physical examination of suspicious lesions with hand-held lighted magnifiers – i.e. Dermoscopes. Oil, alcohol, or polarizing light is used to reveal networks, dots, streaks, etc in the epidermis and papillary dermis, by a ~10x magnification.

^c Not Applicable.

^d This process includes usage of fluorescent dyes, that bind to proteins or DNA, and they emit light after excitation in a certain spectrum.

It should be pointed out that none of the so far reviewed tools seems to provide a means for generating high specificity and conclusive results in classifying between various MM cell-lines. Most methods target to distinguish between benign and malignant lesions, even though the treatment course should be adjusted based on the MM stage. This is defined by the different cell-lines found in MM cancer, like a proliferative-like line, which is found mostly at the first stages of cancer (including local invasion) and a metastatic cell-line found in the late melanoma stages, where the malignancy is more intense.

Impedance-based monitoring (IM) has been successfully adopted as a label-free (i.e. no employment of molecular markers) and optics-free analytical method in recent cancer detection and classification (e.g. breast, skin, prostate [15], [17], [28]). Cancer cells are not-electrically-active cell-types. Nevertheless, they do exhibit electrochemical properties which are distinct from their healthy counterparts in different spectra. Similar distinctions can be found between cell-lines of the same cancer-origin, allowing for classification. IM works on this premise. Technical aspects of Impedance and its Analysis are provided in Chapter 2. Here a brief introduction that correlates Impedance measurements with cancer diagnostics and research is given.

When used for characterization of living-systems, such as cells, impedance measurements correspond to the response of the cell-system-interface after an external excitation signal is presented to the cell [16], [17], [19]. This is achieved with measurements over a wide frequency-range⁵, or on single *sweet-spot frequencies* which are known (or have been tested) to contain information of interest for the conducted research. A current (or voltage) sinusoid – or squared biphasic pulses – is sent from external or integrated electrical-components to the electrodes where the cell is attached, and the voltage (or current) response is then recorded back from the system. The Impedance value can be calculated and further processed either by the system itself online, or with post-processing from offline matlab-scripts. The data are normally obtained with a low-noise and biocompatible (micro)electrode-based setup (i.e. a transducer), offering high-sensitivity and improved specificity to variations over the spectrum.

For MM diagnosis on tissue, commercial EIS Instrumentation with a classification analyzer [23], [28] has the ability to complement dermoscopy and histology examinations by applying an alternating potential between two electrode-bars at the tip of the used probe. The closer to each other, the smaller the depth of the measurement. Hence, the instrument contains multiple bar-electrodes allowing every possible pairing. The retrieved data are then analyzed together with a reference EIS measurement of a lesion-free skin-area. The classifier compares the two responses and the indication is presented to the attending doctor. The responses are indicative of variation on cell-level allowing enhanced sensitivity and specificity. Yet, atypical nevi differentiation from melanomas is an unsolved challenge. Important biological information and processing ability on single-cell level is missing [30]. For single-cell measurements, in-vitro cultured cell-lines (structured in 2D-monolayers) are seeded (i.e. plated) on a transducing substrate of a multi-electrode biosensor, and impedance variations can then be observed with recordings in real-time [19]-[22].

EIS surpasses many of the limitations encountered in other diagnostic techniques, and the ones that remain can be already handled analytically. Measurements performed via non-invasive interfaces and lack of molecular labeling protect cells from cell-death and cytotoxicity respectively; thus, this method allows long-term experimentation which is key for studying cancer progression. At the same time, sufficient single-cell resolution can be achieved with the use of appropriate (i.e. no bigger than the

⁵ In which case IM is called *Electrical Impedance Spectroscopy*, EIS.

cell-size) electrode-size systems. Supplementing Table 1 with the EIS technique shows the EIS superiority in MM diagnostics and research.

Table 1 – Supplement. Malignant Melanoma Diagnostics: Pros and Cons.

<p>EIS on Tissue</p>	<p><i>Commercial EIS Instruments with Classification Analyzers for Tissue Characterization (e.g. Nevisence from SciBase [28])</i></p>	<table border="1" data-bbox="606 459 1409 492"> <tr> <td style="text-align: center;">✓</td> <td style="text-align: center;">✓</td> <td style="text-align: center;">X</td> <td style="text-align: center;">✓</td> </tr> </table> <p>The range of available frequencies allows characterization of both Extra-cellular and Intra-cellular Matrix of the cells (ECM and ICM) since its function depends largely on ion-movements and concentrations, as well as on cellular and junctional membranes [12]. It is low-cost, non-invasive and label-free [16], [20].</p> <p>It is missing single-cell information (ensembled measurement) and thus it cannot provide information on the subpopulations of high metastatic potential to assist choosing a treatment-course. Also, the complex tissue composition may affect its results rendering it inconsistent [19], [30]. That is why it is only used as a complement to other diagnostic methods to characterize a cancerous tissue from a healthy one [18].</p>	✓	✓	X	✓
✓	✓	X	✓			
<p>EIS on single-cells in-vitro</p>	<p><i>Cell-based Biosensors with Impedance Modality</i></p>	<table border="1" data-bbox="606 878 1409 911"> <tr> <td style="text-align: center;">✓^e</td> <td style="text-align: center;">✓^e</td> <td style="text-align: center;">✓</td> <td style="text-align: center;">✓</td> </tr> </table> <p>It is a great tool for cell-line classification purposes and for research on metastatic processes, like cell-adhesion and detachment dynamics [19]-[22].</p> <p>Overlapping of certain system-characteristics (convolution) requires analytical methods with equivalent circuit modeling [27].</p>	✓ ^e	✓ ^e	✓	✓
✓ ^e	✓ ^e	✓	✓			

^e Depends on the system specifications. Depth specificity (single-cell), spatial resolution (high-density (HD)) and reliability (multiple single-cell readout) will determine the final resolution of the biosensor.

In-vitro Cell Cultures

It is common to perform cell-line studies in-vitro, using cultured cells derived from animals or humans. A high-level description of the process of obtaining the cell-cultures is shown in Figure 4. Cells are dissociated from the tissue with a biochemical enzymatic process, and then they are placed in a nutritious buffer solution (cell-medium), inside special sterile flasks (cell-seeding, or cell-plating). The cells will enter as a cell-suspension and then sediment, adhere, and gradually proliferate at the bottom surface of the flask forming a 2D-monolayer of cells. The flasks are preserved in near-physiological settings for ensuring homeostasis (i.e. incubator conditions: 37°C and 5% CO₂). When a certain confluence of the flask's surface is reached, cell-passaging is needed. This involves cell-trypsinization for cells to detach and form a suspension inside fresh medium; eventually portion of this is seeded to a new flask or plated on a chip for experimentation. If a cell-line is *immortalized* (common for cancer lines), according to scientific terminology, it has the capacity for an infinite number of passages allowed by certain mutations. However, in practice, this is not very accurate to say, as no cell-line can proliferate indefinitely. In reality, immortalized cell-lines can simply undergo a rather high amount of passages compared to normal cell-lines.

Melanoma Cell Lines

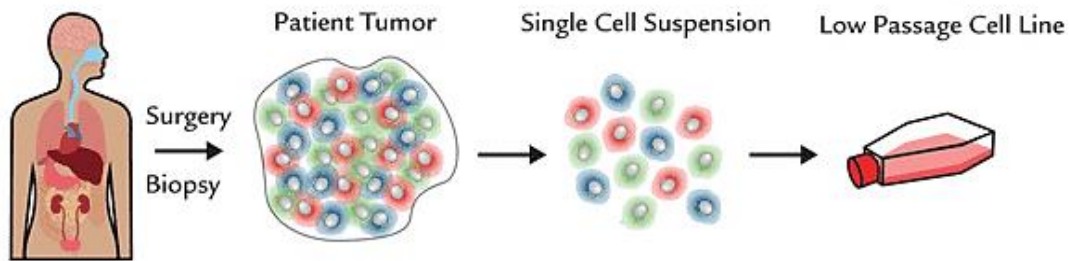


Figure 4. Human-derived cell culture of MM cell-line for future in-vitro experimentation [26].

1.3 Problem Statement

MM cancer exhibits undifferentiated signatures on a molecular level and epigenetic dependency of single-cells. This reveals the existence of minority subpopulations with distinct and dynamic functional and morphological characteristics. Such subpopulations are believed to contain key-information on crucial underlying mechanisms of cancer progression and aggressiveness. Conventional diagnostic tools for the detection of malignancies of the skin (MM cancer) include histological, optical, ultrasound, and impedance-based techniques. Histology and Full Body Tomography (i.e. MRI, or PET scans) are both labelled methods, preventing long-term experimentation due to cell-toxicity and patient safety respectively. Histology's accuracy depends on the obtained sample and its heterogeneous capacity, while for MRI some patients are excluded altogether from testing if they have a metal implant. Optical-based methods and ultrasounds, like Dermoscopy, OCT and high or low frequency Ultrasounds, display a tradeoff between having adequate depth in the measurements (specificity factor) and high-spatial resolution (reliability factor) for clinical classification.

EIS overcomes many of the reported spatiotemporal tradeoffs and limitations for MM diagnosis as a label-free and optics-free analytical method. On tissue level, this method introduces enhanced specificity and sensitivity with measurements that are indicative of cell level variation. Yet, "true" heterogeneity information is masked from the ensembled character of the measurements. Efficient clinical classification between MM cell-lines and understanding of the underlying heterogeneity processes that promote cancer aggressiveness are still unclear. **Important biological information and processing ability on single-cell level is missing.** The necessity for platforms that perform "true" single-cell analysis without omitting the benefit of high density and enhanced spatial (i.e. high-throughput) resolution is essential, aiming to retrieve biological information that has not been addressed efficiently in cancer research before. Such platforms are now available. Multielectrode Array systems have been traditionally used for HD measurements, even though only recently the parallel readout of the MEAs allowed high-throughput recordings. To this date, only one has been published to have 1024-electrode readout for Impedance Monitoring at 2 fixed frequencies and capability for 64 parallel sites of EIS in a 16-frequency spectrum, i.e. [31].

Studying single-cell dynamics over time with a high-throughput system, one can obtain useful information on the heterogeneous subpopulations which are responsible for the MM aggressiveness in different cell-lines. This is not a new theory. However, when combined with a high-density (HD) and high-throughput, label-free bioassay for single-cell studies it may increase the effectiveness in diagnostics for diverse MM cell-lines' classification, and characterization within each line **at the same time**. This project focuses on this novel idea. It aims to investigate experimentally the possibility and

capabilities of such a bioassay development, create working protocols and generate a fundamental basis for analysis and interpretation of the big-data-sets that are derived from using the IM modality [31]. To the best of my knowledge no previous report has been made for such a high-throughput Impedance-based bioassay on diverse MM cancer cell-lines, aiming both for classification, and for heterogeneity identification between and within cell-lines respectively.

1.4 Thesis Structure

Chapter 2 compiles literature information on technical aspects of Impedance, and on the EIS analysis and validation, by using equivalent circuits which model the material-cell interface. The ways Impedance is used in cancer research is also elaborated.

Chapter 3 provides the Experimental Process followed for the bioassay development. It contains the experimental methods (i.e. MM Cell-lines information, MEA System characteristics, Control System Automation Design, Data Processing, Analysis and Validation (Cell-Imaging)) and procedures for achieving the goal of this project. An overview of the experiments to follow is given towards the end.

Chapter 4 contains the Experimental Measurements, their analysis, and main conclusions derived from the results. Discussion on the results is performed per experiment and a conclusion is presented in the end.

Chapter 5 presents a Discussion section and the Prospects after this project. The benefits and potential of the derived bioassay are presented, along with remaining issues and ideas for further development. A novel high-level analysis method is proposed, aiming to introduce another approach for analysis and interpretation of the measurements.

A **List of Abbreviations** can be found after Chapter 5.

The **Appendix** contains the cell-passaging protocol implemented for the two melanoma-cell-lines.

2.

Impedance Spectroscopy for Cell– Analysis

"The only thing I know is that I know nothing."

Socrates

This chapter contains more technical collective information on Impedance and EIS analysis' models and theories for tissues and single-cells. It provides some general equations and graphs that explain mathematically the notion of Impedance as seen in Electrical engineering. Impedance-based cancer progression studies in-vitro (i.e. cell-adhesion and detachment, growth, and motility), and their correlation to biology is conferred further in this chapter. Impedance Spectroscopy (IS) is viewed through the theories in Electrochemistry (on tissue-level). A recognized single-cell equivalent-circuit in an electrode-based transducer setup is presented and analyzed, helping to understand more in depth the contribution of IS and equivalent-model-analysis for the interpretation of single-cell measurements. Commonly used interfaces for in-vitro impedance-based measurements for single-cells are discussed, introduce the Multielectrode Array (MEA) systems.

2.1 Impedance

Electrical Impedance was first studied by Oliver Heaviside in 1880s in the field of electrical engineering [38], [39]. Impedance measurements illustrate the voltage and alternating-current relation as an extension of Ohm's Law in the complex plane, since phase variation is considered (Figure 5).

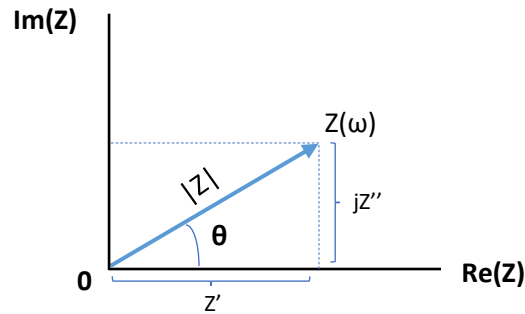


Figure 5. Impedance in the complex plane: Argand Diagram.

Impedance can be viewed as a vector in this plane that contains a real and an imaginary component. This representation is used for systems that show both resistive (i.e. resistance) and capacitive (i.e. reactance) behavior. In semiconductors the lack of magnetic field variation excludes inductive behavior from the reactance. Equation (1) shows the rectangular coordinates' representation:

$$Z(\omega) = Z' + jZ'' \text{ [Ohms]} \quad (1)$$

, where $Z' = \text{Re}(Z(\omega)) = |Z| \cos(\theta)$, $Z'' = \text{Im}(Z(\omega)) = |Z| \sin(\theta)$, $j = \sqrt{-1}$, and ω represents the angular frequency that relates to the frequency with the equation: $\omega = 2\pi f$ rads/ sec. *Theta* (θ) is the phase angle between the voltage and the current, measure in degrees. For a resistor, $\theta = 0$, while for an ideal capacitor, $\theta = -90$. Equations (2) and (3) are defining the magnitude and the phase of the Impedance vector in Polar coordinates:

$$|Z| = \sqrt{(Z')^2 + (Z'')^2} \quad (2)$$

$$\theta = \tan^{-1}\left(\frac{Z''}{Z'}\right) \quad (3)$$

Consequently: $Z = |Z| \angle \theta \quad (4)$

From the capacitive element, one can conclude that impedance is frequency dependent and thus, it can be used to characterize different material properties over a relative frequency-range. More details are given in following sections.

2.2 Fundamentals of Electrical Impedance Spectroscopy in Cancer

Impedance Spectroscopy (IS) is a common method used to characterize materials and systems over a wide frequency-range. In cell-based biosensing, like the experiments conducted in this project, the characterization refers to the cell-electrode-electrolyte conjunction. In impedance sensing a small AC excitation signal (frequency-dependent and usually sinusoidal) is applied to the electrode-cell interface and the response is measured. The capacitive and resistive components of the system will delay the current through the device. By measuring the phase-delay and the voltage, Impedance can be calculated via the equations in 2.1 [20]. The excitation is big enough to perturb but not alter the system's characteristics in any way.

In cancer research, Impedance Spectroscopy has been used successfully to investigate metastatic or apoptotic (i.e. self-cell-death) mechanisms of the cells on single-cell level; such are cell-growth, adhesion, motility and detachment. Relevant studies and reviews – i.e. [19]-[22] – use impedance measurements with in-vitro cultured cell-lines structured in 2D-monolayers. These are seeded (i.e. plated) on a transducing-substrate and impedance variations can then be observed with recordings in real-time. The obtained measurements are frequency-, buffer-, and cell-type-dependent. In other words, the derived impedance will characterize diverse parts of the cell-system-interface for the different frequencies, cell-types, and cell-medium conductivities.

High-frequencies above 1MHz may cause the cell's capacitive demeanor to drop or short and alter the system's behavior to be resistive (intracellular information on the cell's cytoplasm); middle frequency-bands of about 1kHz to 100kHz infer mostly on the sealing-Impedance of the cell-electrode interface (i.e. resistance of the buffer – cell-medium – trapped in the cleft between the cell and the material) [20], [27]. This varies with deviations of the cell's distance from the electrode or changes in the cell's spread over the electrode. This is why it is the most interesting band for studies on cell-adhesion and detachment-dynamics. Finally, lower frequencies are highly dependent on the transducing material and tend to provide information on the electrode's double-layer capacitance.

In Chapter 1, it was reported that cells vary between different tissues (or within the same, i.e. intratumoral heterogeneity) in morphology and functionality. Since EIS provides in some frequencies information on these physiological and anatomical (cell-size, cell-morphology, etc) characteristics, the electrochemical response of the system on impedance level will also be affected by them. The cell-medium conductivity, will also affect the total system's measurement as well as for certain frequencies in which the electrode-electrolyte interface response is mainly measured. That is why, every time cell-types and media are altered in a given transducing system, new characterization over the spectrum is suggested.

The benefits of having this type of information extracted on single-cell level for many cells of an adherent cell-line, can show both a high-resolution average-response (used mostly for classification) and the variance within the population of cells for heterogeneity investigation. The prospects of such a method, combined with efficient transducing electrode-layouts are immense: clinical biopsies, personalized-treatment with in-vitro drug-testing, research-relevant biological information for understanding better the metastatic processes of cancers, are a few of the potential uses.

However, there are still some disadvantages with using the IM method which need to be reported. One is the partial overlapping of the different system-characteristics for some frequencies (see an example in Figure 6).

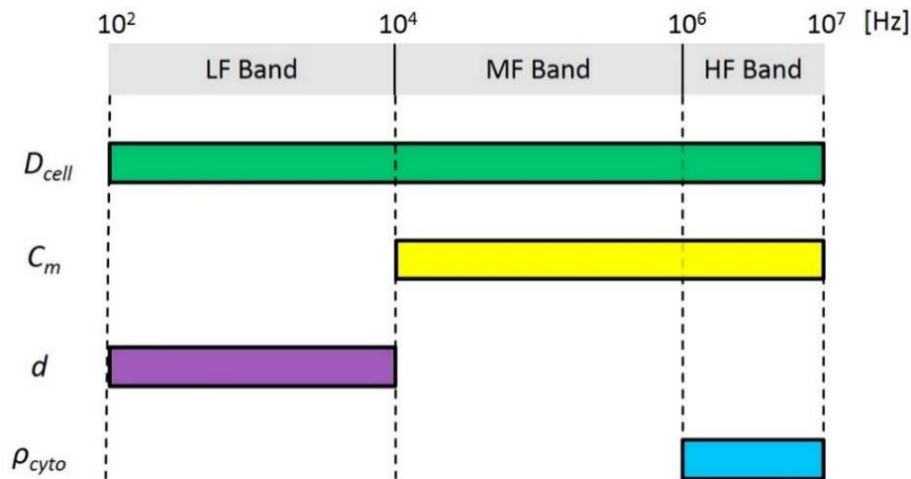


Figure 6. Example of cell-electrode-electrolyte characteristics overlapping in the spectrum [27].

LF: Low-Frequency band; MF: Middle-Frequency band; HF: High-Frequency band. D_{cell} is the lateral diameter of the cell as it spreads over the electrode surface; C_m is the membrane capacitance of the cell; d is the distance of the cell from the electrode (cleft) which change provides information on the Sealing Impedance; ρ_{cyto} is the conductivity of the cytoplasmic solution inside the cell's membrane.

This is why the analysis of the obtained results includes equivalent-circuit modeling and corresponding mathematical expressions which describe these changes over the spectrum in a more defined way. The circuit models are simulated in special programs that contain simulated spectrum-analyzers, and the experimental data are fitted into the model. This way, other components that have not been considered may surface from the fitting, or a research may be validated when the data fit the model's response over the spectrum. Having seen how a cell-line can affect the impedance values for different frequency bands, it is important to perform at least once a full spectrum measurement per cell-line for a given system, to localize the sweet-spot frequencies that provide the desirable-feature information. A few examples of commonly encountered models for the EIS analysis are provided in the next Section.

2.3 Equivalent Circuits and the Cell-Electrode Interface

2.3.1 Equivalent Circuit: Electrode-Electrolyte Interface Model

Based on Electrochemistry, when a solid (i.e. a metal in our case, the electrode) is immersed into an *electrolyte*⁶ the phase on either side of the boundary becomes equally and oppositely charged (electrons transfer), generating a potential difference (causality: redox reactions). Helmholtz suggested that the potential is created in the form of a two-layer charge-accumulation (of opposite polarity) in two close-proximity parts of the system: the electrode's surface and the bulk of the electrolyte [41]. This double-charge-layer behaves like a capacitor and gives to the interface a relative component termed *double layer capacitor*, C_{DL} , or *Helmholtz capacitor*, C_H . However, the capacitive behavior is not ideal; there is some leakage of charge across the double-layer; this is representing the

⁶ Electrolytes are solutions where ions are the charge carriers. For this project, as electrolyte is considered the cell-medium.

exchange of electrons between the electrode and the electrolyte and it is given the form of a resistor called *charge transfer resistance*, or *Nernst Impedance*, R_{ct} . The field accelerates the already occurring oxidation (loss of electrons) and inhibits the reduction reaction (gain of electrodes) leading to a final equilibrium of zero net-current. Diffusion of ions due to thermal motion along with galvanic processes was explained by Gouy-Chapman. Yet, both models fail to fully describe efficiently the system when they are used individually. Stern's C_{DL} theory combined both Helmholtz' and Gouy's theories. He separated the system to two areas: the Stern/Helmholtz (Inner HP) layer and the (Outer HP) Gouy-Chapman [24], [37], [40]-[42]. Figure 7 shows the different Models.

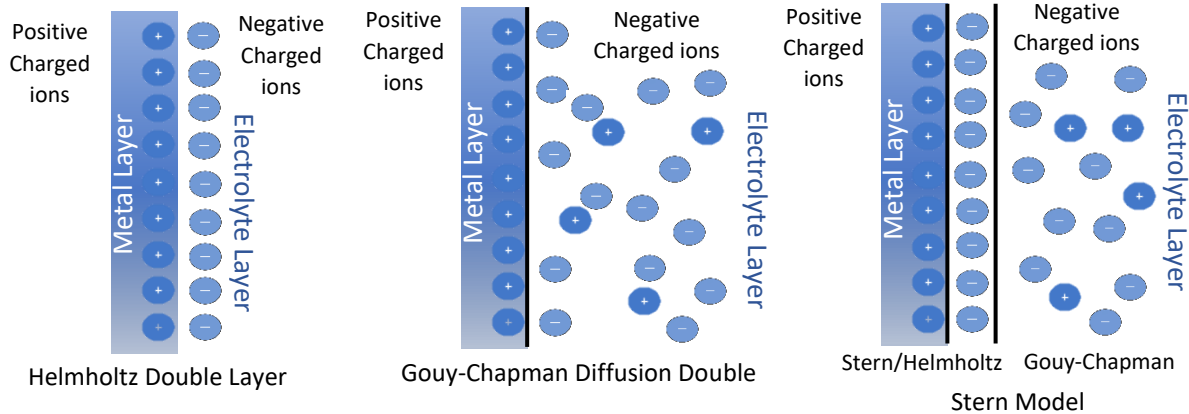


Figure 7. Double-Layer Capacitance (C_{DL}) Models: Helmholtz, Gouy-Chapman, and Stern Models.

The corresponding capacitances' equation: $\frac{1}{C_S} = \frac{1}{C_H} + \frac{1}{C_{GC}}$, where C_S (Stern's double-layer capacitance), C_H the capacitance of the outer Helmholtz and C_{GC} the capacitance of the diffuse layer [40]. According to this model, the interfacial Impedance has two in-series, resistive components: the one caused by the charge-transfer (IHP) and the one caused from the Gouy-Chapman diffusion (OHP). The given names are the charge-transfer R_{CT} and the Warburg (Z_w) impedance seen in Figure 8. The rest of the electrolyte (called the *bulk*) is inserting a resistive response in series to the parallel configuration of the actual interface.

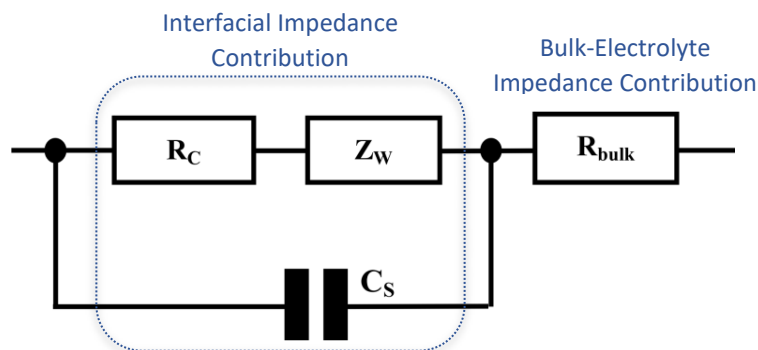


Figure 8. Standard Equivalent-Electrical-Circuit: Electrode-Electrolyte Interface [40].

In recent studies [20], [22] [46], the Warburg Impedance is omitted, since experimentation proved its existence does not affect the overall impedance. The double-layer's capacitive behavior is not always pure, due to a small leakage. Hence, C_s is replaced by a theoretical component, known as *Constant Phase Element* (CPE). The CPE's equation can be seen below (Eq. 5):

$$Z_{CPE} = \frac{1}{(j\omega)^\alpha} \quad (5)$$

, where α is a constant $\in [0.6,1]$. It takes its value according to the frequency and the system. When it is equal to 1, the CPE element is a pure capacitor. The R_{bulk} , is referring to the solution of the electrolyte, and it is commonly addressed as R_s . Then, the equivalent circuit of the electrode-electrolyte Interface (Figure 8) takes the form of Figure 9.

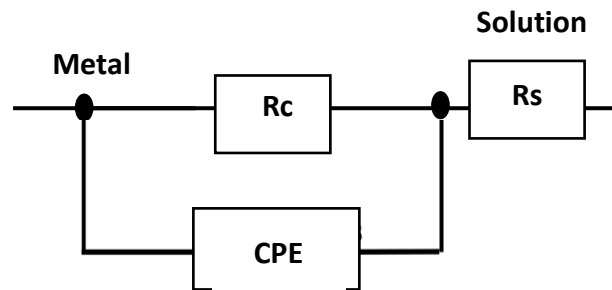


Figure 9. Standard Equivalent-Electrical-Circuit accounting for impure capacitive behavior expressed by the double-layer capacitance: Electrode-Electrolyte Interface with CPA element and no Warburg Impedance. Based on the graphs in [40], [46].

In this context, electrode-material interfaces of semiconductors can be viewed as simple equivalent-circuit models comprised of resistors and capacitors. In Section 2.1, the frequency-dependency of such systems was concluded. These frequency-based changes in impedance are mostly determined by the electrophysiological-characteristics of the interface, as well as by the current that is injected to perform the measurement in the first place. Modeling a biological system in this way, may seem as an oversimplification of all the complex electrochemical processes that take place in reality; however, it has been proved that efficient modelling of the distinct behaviors of the components over the spectra is achieved. EIS is often found in bibliography as an *electrode-electrolyte interface characterization* or an *electrode-tissue interface characterization* technique.

2.3.2 Equivalent Circuit: Tissue-Model

Around the 1920s, EIS was introduced in research for biological systems. This method can simulate with passive electrical components (i.e. resistors and capacitors) the biological behavior of a sample if it can be affected electrically (e.g. cell-membrane, intra- and extra- cellular fluids, interfaces with the electrolyte, etc) to produce a response. Fricke proposed a rather simplified circuit to emulate tissue-responses; it depicted the intra- and extra-cellular analytes of the cell with resistors – R_i and R_e respectively – and the cell membrane with an ideal capacitor – C_m (Figure 10) [16].

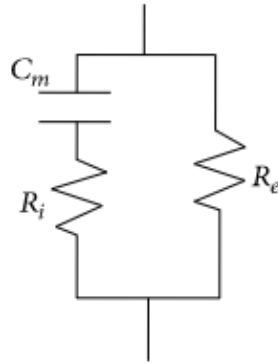


Figure 10. Fricke's Model

All three parameters of the model are ion-concentration and mobility dependent and can reveal the tissue's physiochemical properties. Extensive experimentation deemed necessary to augment the model in order to simulate more realistically the system-response. An electrode-tissue interface evokes non-linearities in a real-life setting. This relates to a phenomenon called *Dispersion*, also known as frequency scattering causing radical changes to the parameters. Schwan localized it for biological systems in 3 different frequency-bands, each representing one dispersion (α, β, γ). Hence, C_m was replaced with a CPE element, like in the Electrode-Electrolyte Interface to account for dispersion.

Fitting techniques are often used for two main purposes: (i) to determine how well the equivalent model behaves similarly to the physical system; and (ii) to validate later experimental results of added complexity. Single-cell models include a microelectrode-electrolyte interface as well as a cell-material interface and have been used a lot in single-cell EIS studies for fitting the experimental data and interpret them.

2.3.3 Equivalent Circuit: Single-Cell on-Chip Model

From tissue to cell, the aforementioned processes are extended. In this sub-section, two recognized equivalent-circuits for the single-cell interface with a flat transducing surface, are reviewed. Multielectrode Array transducers are used to unlock the full potential of IM methodology in cancer research and diagnostics. Hence, the combination of the cell-(tissue)-electrolyte and electrode-electrolyte models, will provide the complete equivalent circuit of the cell-electrode-electrolyte interface, used for in-vitro cell experimentation. An introduction on MEAs is given after this section.

Cells are conventionally modelled the same way, while the interface-components for the electrodes may differ based on the type of the transducer (flat, grooved, etc) and the effect of the parasitic capacitance to the overall Impedance. Below, two examples of different transducers are presented (Figure 11).

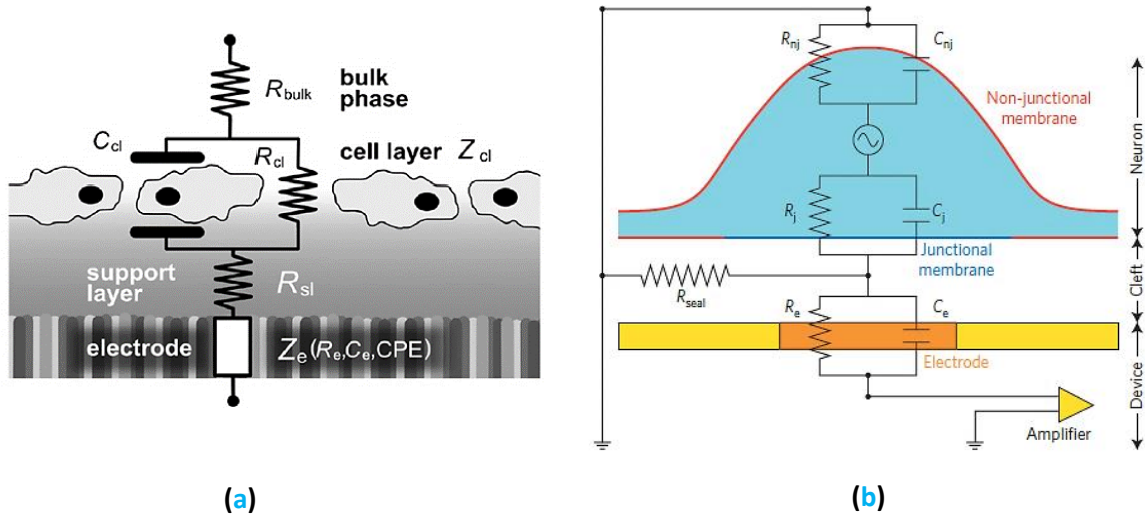


Figure 11. Flat-Electrode Systems, Single-cell equivalent-electrical circuits (Electrode-Electrolyte-Cell Interface) [47],[48]. (a) ECIS substrate; (b) MEA-electrode substrate.

The cell-membrane is modeled by a capacitor in parallel to a resistor due to the membrane's double-layer characteristics (i.e. is a phospholipid bilayer) in both cases (C_{cl} , R_{cl} and C_j , R_j). The electrode-electrolyte interface is modeled as was depicted before in Figure 9, again for both cases (C_e , R_e , CPE and C_e , R_e). It is noted that for the MEA substrate, the CPE element is not depicted. Similarly, the sealing resistance (R_{sl} and R_{seal} , indicative of cell-adhesion on full electrode) is modeled between the electrode and the cell (in the cleft). The main differences are the interface-components for the cell-(bulk)electrolyte interface, since in the MEA system, this is depicted with an RC again only of different values (R_{nj} , C_{nj} and the R_{bulk}).

Now the description given in Section 2.2, for the responses of an electrode-electrolyte-cell interface over different spectra bands, proves the observations drawn: low frequency regions along this frequency range will provide information of the electrode's electrochemical responses (CPE has low capacitance); middle frequencies indicate the cell-adhesion on the surface through the sealing impedance and electrolyte responses (current is perturbing the solution between the cell and the electrode, R_{seal} , but not the cell-membrane capacitance as C_m is very high); while towards the higher frequencies, information for the intra- and extra-cellular morphology will prevail (C_m is leaking). Below are three indicative studies that illustrate in experimental settings, how EIS can answer different research questions. This is shown to demonstrate the extend of information one may obtain by using EIS with cells: e.g. drug-testing and metastatic potential, clinical classification, clinical biopsy. The potential is immense.

In 2010, L. Arias et al. validated the EIS method as a powerful and label-free detection and characterization method for cellular activity, in real time settings [49]. The study used Oral Squamous Cell Carcinoma (OSCC) cells and monitored their impedance behavior between intervals of 5 up to 30 minutes. Cell adhesion as an important factor of cancer metastasis, and responses to anti-cancer drugs were studied. Impedance-based cell index related cell proliferation and spreading to impedance values. A higher cell-index corresponds to higher impedance values and to more electrode coverage.

However, this correlation is only valid for the cases where the cells cover more than 10% of the electrode's surface. When cancer cells were treated with cisplatin, a drug, cell apoptosis was initiated after a time period which relates to the drug's concentration. With cell apoptosis, reduced the impedance-based cell index as well. Due to its sensitivity, impedance-based cell-index was proposed as a possible, label-free detection system of circulating CTCs, which may serve as an indicator that correlates clinical stage of the cancer and tumor metastasis.

In 2013, H.G. Jahnke et al, presented a self-made instrumentation, of a 32-TiN-electrode array, biocompatible and flexible for an in-vivo rat model study on Glioblastoma differentiation from normal brain tissue, using the EIS method [50]. Main methods used, involved the characterization of the system itself – i.e. electrode-material interface, by dipping it in PBS. The values of the tumor were normalized over the normal tissue values for every subject/rat. This way, the statistical analysis would be more comprehensive. Furthermore, an equivalent circuit was used to gain extra insight for the nature of the specific spectra characteristics that was studied or was indicated interesting. Main findings showed that for the normal-tissue measurements, between the frequencies 100Hz -500 kHz, a plateau was observed (possibly to indicate the prevalence of R_{seal}). On the other hand, the tumor never indicated such plateau. Last but not least, a reference to the loss of adhesion for the tumor cells was made (initiation of metastasis), in order to connect and justify the decrease observed in the extracellular-environment of the tissue (R_{extra} is reduced). Significant distinction between malignant and benign regions was observed in the frequency range: 10-20kHz.

In 2013, P-J. Chao et al. proved the effectiveness and of an EIS system for usage as complimentary monitoring technique in a clinical environment [51]. The aim of having EIS as an aid, was to assess the possible tissue damages, caused by irradiation for malignancy treatment. Rats were the biological model to use in this study. The tissue was modelled with a standard, simplified three-element (RC) model in order to validate the useful biological information from the EIS measurements. The frequency-range for the measurements was given between 10kHz and 100 kHz. One of the main observations in this study was that EIS variations correlates to morphological divergence. Thus, EIS would be a great tool to differentiate between those changes and the non-pathological ones. This concept, was first introduced in 2011 as “electrical biopsy” for aiding diagnostics.

Reported in the previous section, single-cell impedance measurements are conventionally performed with the aid of microelectrode array (MEA) platforms. Due to the limited throughput of MEA systems and the need for bulky readout equipment, recent developments have led to the design of high-density (HD) CMOS-MEA systems with more than 1000 sensing sites and integrated readout electronics [31], [32], [33]. These platforms have enabled us to equip them with novel bioassays and study single-cell cancer-models like MM with increased mutations. An Introduction to MEAs and their use in in-vitro experimentation with cells, is given in Section 2.4.

2.4 Multi-Electrode Array Systems for Single-cell Assays & Analysis

2.4.1 An Introduction to MEA systems

Microelectrodes can be a stable and non-invasive, biocompatible-interface for monitoring over extended periods of time the electrical properties of a cell-population (i.e. cell-culture) in-vitro. MEAs constitute an arrangement of micro-electrodes that allow extracellular recording and stimulation by targeting multiple sites in parallel. Initially, single transducers allowed a readout of a single-electrode at a time. However, MEA technology has evolved a lot after the 1950s, when multiple transducers were included in the design to increase the readout to multiple electrodes. Available for commercial use came to be only in the late 1990s, while before they were found in academic and research facilities. Primary cells and cell-lines are positioned directly on top of the active electrode-area. With proper packaging (i.e. glass/PDMS-based ring, insulation of wirebonds and carrier-PCB surface with biocompatible materials), MEAs serve as a culture-chamber ready to be thoroughly tested with the provided *modalities* (i.e. diverse channels for different measurements and stimulation protocols) [34]-[37]. Figure 12a demonstrates the logical-architecture of a Multi-modal MEA; and Figure 12b illustrates a different example of a packaged MEA ready to use in cell-experiments.

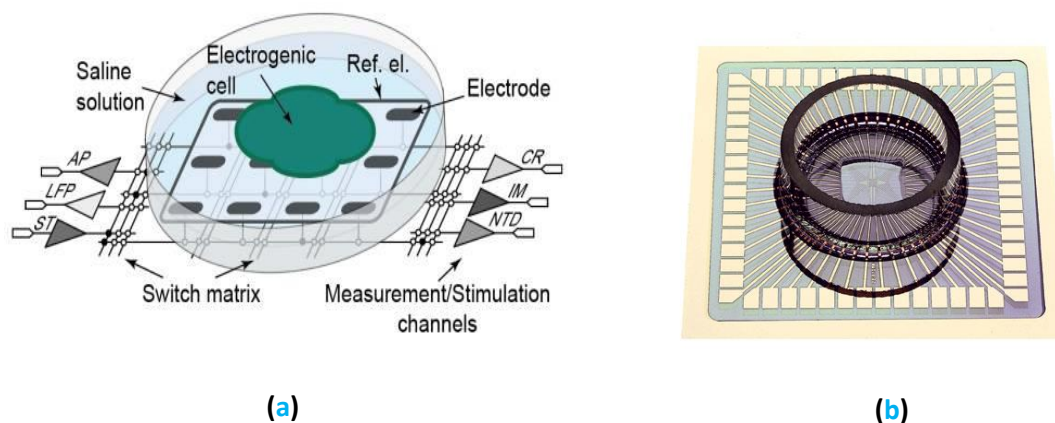


Figure 12. (a) Example of an active HD-MEA chip with an electrogenic cell on top of the active electrode-area and multiple modalities (high-level picture and low-level architecture examples) [32]; Switch-Matrix-based system showing multiple modalities of the system (i.e. Action Potential readout (AP); Local Field Potential readout (LFP); Current Readout (CR); Impedance Measurement (IM); Neurotransmitter Detection (NTD); and Stimulation (ST) channels), (b) Example of a non-active packaged MEA on a carrier-PCB with a ring-chamber ready for use with cells [IMEC©Copyright].

2.4.2 Plating cells on MEA transducers for experimentation

Conventionally, human- or animal-derived cancer cell-lines (process shown before in sub-Chapter 1.1.2) are (*sub*)cultured in incubator conditions until there is necessity for experimentation on the available biosensor. Taking the example of human-derived MM cell-lines and a MEA system biosensor; The cells are kept adherent on the flask's bottom (e.g. T25 flasks). To extract and transfer them to the transducer's electrode surface, a certain procedure is required. This is illustrated in Figure 13.

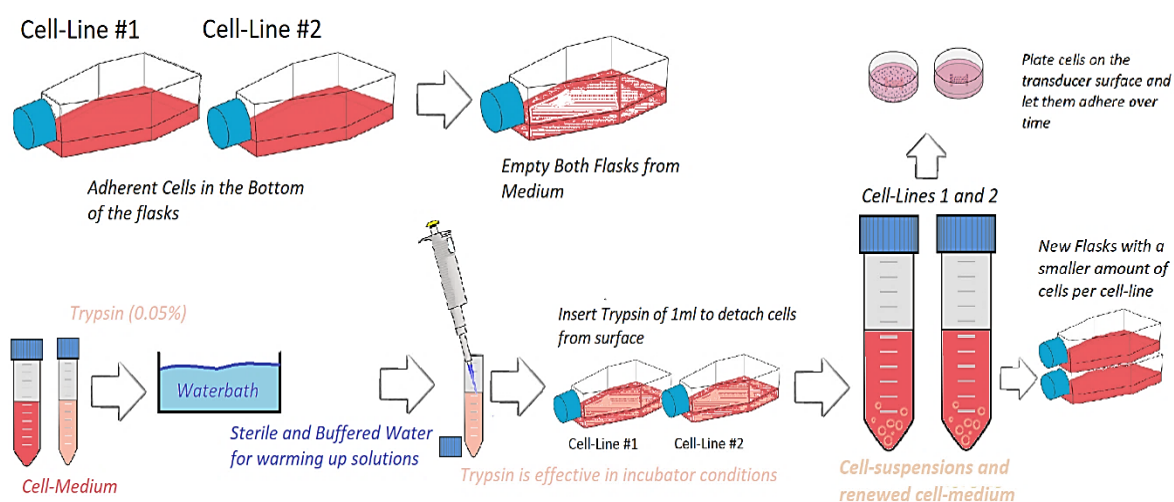


Figure 13. (Sub)culturing and plating on-chip (transducer) process.

*Trypsin*⁷ (0.25%) from stock is warmed in the water-bath (~37°C) and then diluted to reach 0.05% concentration for the culture with HBSS buffer (i.e. a balanced salt solution), deprived from Calcium and Magnesium. Having removed the cell-medium from the flasks, 1ml of the aliquot is inserted per cell-line and each flask placed in the incubator for ~2min to act. The cells' condition is checked under the microscope and when detachment is noticed, Trypsin is neutralized with ~4ml of cell medium. This creates a 5ml cell-suspension per cell-line ready to split and seed in other flasks, or on the transducer. Plating-time is called *Time-Point Zero* (i.e. 0hrs) and IM measurement on the cells can commence from that time onwards. For the cells to adhere properly, either a coating is applied prior to plating on the layout of the electrodes, or the chip is UV-Ozoned for at least 15 minutes (after sterilization), to drop its impedance and hydrophilize the material. A cup is placed over the ring on the chip to ensure sterility and the plated cells are transferred into incubator conditions until the experiments takes place.

⁷ Trypsin is a protease creating an enzymatic-reaction that detaches the cells from their Extracellular Matrix and if left for long, creates pores on the cell-membrane, killing the cells. In dilutions is used for cell-culturing.

2.3.4 MEA Modalities and Data Acquisition-and-Processing

Microfabrication processes and CMOS technology are the bases for MEA systems' development. The systems may be active or passive, depending on whether they have integrated transistor-based electronics or not. Very few systems to this date have more than 4 modalities, since HD systems with high reconfigurability started to surface the past decade alone. Those are called Multi-modal MEA Systems and are capable to shift between different modes (current or/and voltage stimulation, recording, EIS recording, Impedance Monitoring over time for fixed frequencies, etc). Researchers and CMOS designers, ideally would like to integrate such modalities all in a single MEA that is fit for high-throughput experimentation (i.e. advanced parallel-channel readout). In this project, such a system is used and its main characteristics will be presented in the methods, in Chapter 3.

The integrated microsensors benefit from *Micro-Electro-Mechanical Systems (MEMS)* technology. This has even allowed for simple signal pre-processing (i.e. amplification and filtering), or Analog-to-Digital (ADC) and Digital-to-Analog (DAC) conversions for the diverse (bio)sensor interfaces, on-chip. However, the biggest part of processing and analysis is performed mostly offline, using data-analysis environments. An interface for receiving and transmitting data and the controls is always included as part of a complete experimental setup.

To retrieve the Impedance Information from the chip, normally an I/Q Demodulator is used [53]. As the AC current passes through the interfacial Impedance, it gets distorted, delaying in its response, and then, Ohm's Law guides the creation of a complex voltage signal (V_{in}) at the output of the interface. Information on the Impedance real and imaginary components is hidden within the amplitude and the phase of the retrieved voltage. Often, low-noise amplifiers are used to enhance the signal (as it may be rather small). The complex value is sent to two separate paths and that mix the signal with an In-phase (I) and a Quadrature (Q) local oscillation (LO) signals. In-phase signal contains the ideal phase of the injected current, while the Quadrature normally is set to +90degrees shifted. Modulation of the voltage at a higher frequency occurs to transform all the impedance information to DC signals, which are digitized through ADC components to read out. Then $Z = I + jQ$.

Having understood all the different aspects involved in experimenting with cell cultures on HD and high-throughput MEA systems, using Impedance-based measurements, the following Chapter will provide the Experimental Process followed in this project.

3.

Impedance-based Bioassay

"Design is not what it looks like and feels like.

Design is how it works."

Steve Jobs

In this Chapter, the methods used for the bioassay development are presented. Information covers the following domains: cell-lines used and cell-preservation conditions; the MEA-System used and the Control-Automation designs that were created in the process of the bioassay development; and the basic Data Processing and Analysis used for the results interpretation and validation (i.e. extraction, normalization, statistics, plotting, confocal imaging characteristics).

3.1. Methods & Systems

3.1.1 Cell-Cultures: Malignant Melanoma Cell-Lines

Two human-derived, MM immortalized cell-lines (MM087 and MM029) were obtained from the University Hospital *Lemmensinstituut of Leuven*, Belgium, to use in the experimental process of this project. Their characteristics and drug-resistiveness to common melanoma-drugs were studied in detail in the past, and their strong metastatic potential and poor classification, was the reason they are studied in this project. The MM087 is a wild-type⁸ and it exhibits the BRAF⁹ gene (i.e. WT-BRAF) which is highly prone to mutations. It has proliferative-like behavior with intense dendritic expression (i.e. branched protoplasmic extensions), as can be seen in Figure 14-a. The MM029 cell-line on the other hand, is a BRAF&MEK¹⁰ mutated metastatic cell-line forming droplet-like shapes and completely deprived of dendrites (Figure 14-b). Their difference in morphology, can be used for the IS classification, as in medium-band frequencies some information on cell-morphology is affecting the measurements. Average cell-diameter for both cell-lines has been found experimentally through imaging to be 20 μ m +/- 4 μ m (mean +/- SD).

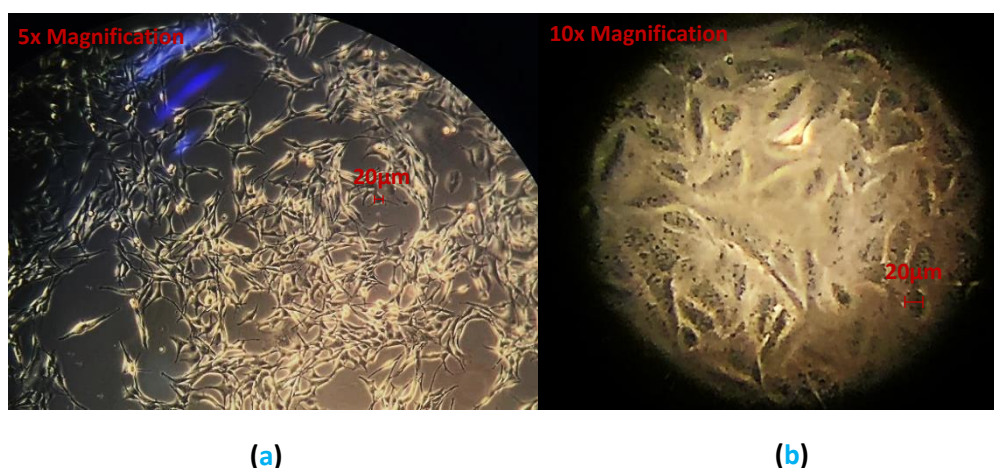


Figure 14. Melanoma Cell-lines: (a) Proliferative MM087, (b) Metastatic MM029.

The cell-lines in Figure 14 were imaged with 5x and 10x magnification-objectives respectively, using a common inverted-microscope. Passaging of each cell-line was based on their proliferation rates which in-average required a follow-up of two times per week. The seeding of the cells on-chip has been performed timely for the type of experiment, after sterilizing and hydrophilizing the chip surface. The cell-protocols followed in this project, can be found in the Appendix. The medium-composition for both cell-lines is a standard Ham's F-10 Nutrient Mix (*ThermoFisher*), supplemented with: 10% FBS for providing the cells with organic enhanced proteins and nutrients, and with 1% Pen/Step as antibiotic protection against infections. The cells were retained in flasks with a breathable cup, inside a cell-line-specific incubator, in sterile conditions of 37°C and 5% of CO₂.

⁸ A Wild-type (WT) cell-line exhibits the most common phenotype for the particular cell-line category. It is the opposite of a mutated-line, even though (BRAF)genes in the line may result to future mutations over this gene.

⁹ BRAF: A gene involved in signaling pathways that regulate cell-growth. Also known as Raf proto-oncogene.

¹⁰ MEK: A mitogen-activated protein Kinase Kinases Enzyme. Is involved in crucial signaling pathways for metastasis.

3.1.2 MEA Platforms: Prototype HD CMOS-MEA System

The main platform adopted to perform single-cell EIS Analysis for the MM cell-lines was a HD CMOS MEA system, developed in IMEC, Belgium [31]. Another passive version of the chip was used with a commercial system (AutoLab) for validation reasons. Information on the latter can be found in Section 3.1.3.

The active system features 16 wells subdivided in 256 pixels per well, with 4 electrodes each (Figure 15). This 1 by 2-centimeter chip allows for simultaneous single-cell stimulation and electrical recording with 1024 parallel channels. Its CMOS-based array and unprecedented channel-readout enhances its capabilities for generating diverse bioassays on various non-active cell-types (e.g. MM cells).

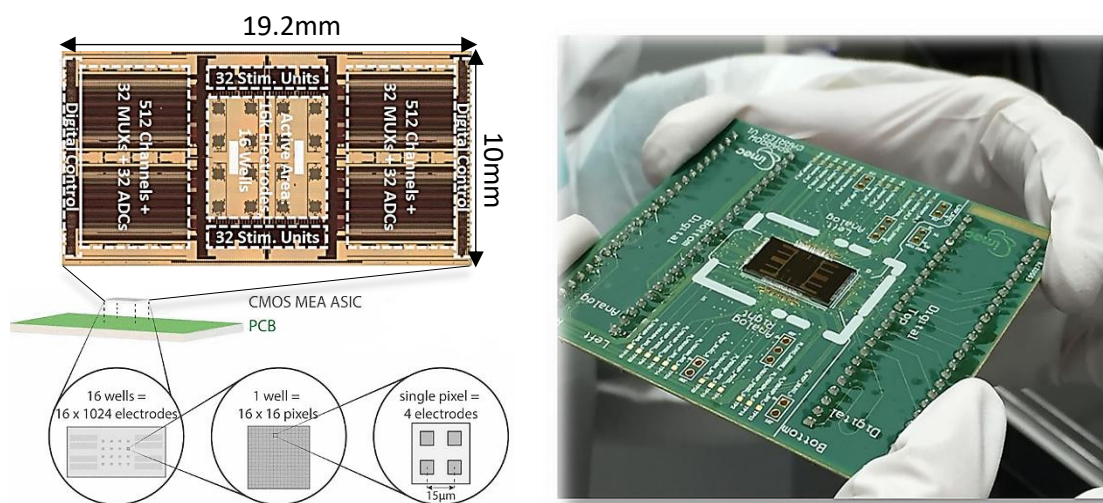


Figure 15. HD-CMOS MEA [31].

Techniques like high-selective electroporation, fast Impedance Monitoring (IM) at 1kHz and 10kHz, and Electrical Impedance Spectroscopy (EIS) over 16 frequencies can be used with this system, for DNA transfection, drug testing, classification, and heterogeneity studies, that may require high selectivity and specificity. According to the Well number, different electrode-sizes can be encountered (i.e. $11 \times 11 \mu\text{m}^2$, $6.5 \times 7 \mu\text{m}^2$, $4.5 \times 4.5 \mu\text{m}^2$, $2.5 \times 3.5 \mu\text{m}^2$); Wells 1 and 2 contain each 64 electrodes from each size, and Wells 3 and 4 contain only the $2.5 \times 3.5 \mu\text{m}^2$ size each. Each Well has 256 electrodes in total. The pitch between pixels is $30 \mu\text{m}$ and between electrodes is $15 \mu\text{m}$.

The Application Specific Integrated Circuit (ASIC) is wire-bonded on a carrier-PCB as seen in Figure 15 and interfaces with external components through its motherboard-PCB. These components include: (i) a battery for generating a biasing dc-voltage and an acrylic electrode grounded to the board - to be used as external reference; (ii) a dc-voltage power supply of 1.2 V, used to power up the electronics; (iii) a pulse-generator to provide the master clock (96MHz); (iv) the Control System and GUI out of the National Instruments (NI) PXI-PC. The schematic of the system is depicted in Figure 16. The control system and the GUI are implemented with LabVIEW 17.0.

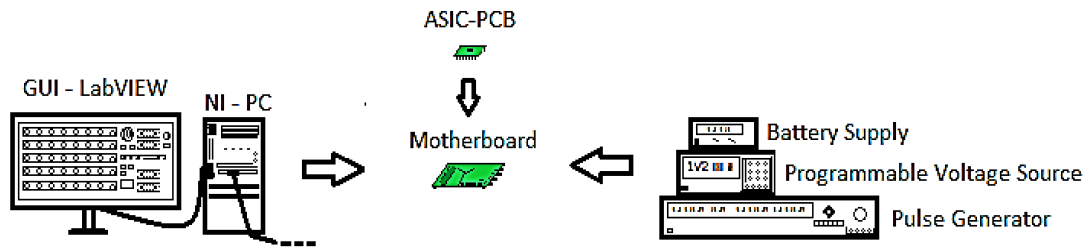


Figure 16. The System.

Specifications: IM and EIS Modalities

During the EIS Measurements (10Hz to 1MHz), the 64 Stimulation Units (SUs) of 8 bits can be controlled and configured individually for Impedance measurements in diverse pixel-configurations. The current-range is 10pA – 384nA. Three end-user protocols for the configuration of the controls of the chip (GUI) are provided. These permit the user to obtain the In-Phase (I), the Quadrature (Q), and the chip-offset components of the configured pixels (maximum 64 electrodes) for offline magnitude and phase extraction. The magnitude and stimulation polarity of the biphasic pulses used in this modality can be controlled individually per pixel (and electrode) globally.

For the IM measurements (at 1kHz and 10kHz), two current amplitudes (internal current sources) are available to use: 1nA and 10nA. These can be configured globally from the GUI in the NI Computer and are expressed in form of square waveforms. A single measurement reads 1024 electrodes (one electrode per pixel per measurement) of one Quadrant in the chip and provides a single data-file to be used in the offline impedance calculation. In this project, the 1nA was used for the 1kHz and 10kHz. The phase of this modality could be reliably extracted from the measure value, and thus the System in 3.1.3 is used instead to validate that the retrieved information lies around the R_{seal} at 1kHz. Amplifiers internally, allow low-noise current amplification with a gain of 50 (i.e. IM final current: 0.5nA).

In both modalities, the control configuration is implemented through a UART port, while the data transmission occurs through a Parallel Synchronous Bus (PSB). The output raw-data are I/Q signals coming from an on-chip processing unit; they are saved in *.bin* format and need extraction with Matlab scripts. The ADC resolution is 10bits and the sampling rate per channel is 30kSPS. The acquisition time determines the number of samples per frequency; usually 2, 5 or 10 seconds are chosen, because temporal resolution is important and, regardless, prolonged sampling (>10sec) will not provide more reliable values.

Control-system Design: IM & EIS Automations

Part of this work involved automating the measurements for the two impedance modalities. The need for the Automations are attributed to the limitations introduced by the prototype. These limitations were observed in the first steps of the experimentation process.

The end-user protocols for **EIS measurements** are extensive and were complemented by a complex GUI environment reducing the modality's temporal resolution. Cells require incubator-conditions to sustain homeostasis which should not surpass the time-range of 15-20minutes. Hence, the resolution of 1 hour (min) and 1 and a half hours (max) for in-vitro, room-temperature experimentation with EIS,

will provide less accurate and replicable characterization. In addition, the DACs used for stimulation would require a change in the current-amplitude given per frequency to ensure enough power is provided to perturb the cell-electrode-electrolyte interface (without saturating the signal). Still, to calibrate, no procedure nor any automated process existed in the prototype control system, necessitating considerable manual work every time a new cell-type is introduced to the system.

Impedance Monitoring on fixed frequencies worked fast (3 minutes per single frequency experiment, for 1024 electrodes) and in an intuitive way (short end-user protocols) despite the complex GUI environment. However, for over-time experiments, no automation procedure existed to allow the end-user hands-off the system and error-free measurements. For extracting all 4 electrodes' information (a total of 4096 data points instead of 1024, with a smaller pitch – enhanced spatial resolution) the experimental time was rising to ~10 minutes per frequency.

For **both modalities**, glitches in the recording process due to the prototype-character of the setup, often added up to increase time and reduce the result's reliability (i.e. conclusiveness) of an experiment.

In this context, the following automated processes were incorporated in the Control System Design to achieve faster and more reliable recordings:

1. IM Automation

A user-friendly control-interface was designed in *Labview Development System* (Version 17.0, of *National Instruments (NI)*, USA) to perform automated impedance readout from 4096 electrodes per measurement (includes now all four electrodes per pixel). An additional feature in the IM automation allowed for flexible time-lapse measurements to be performed during incubation. The latter feature was not fully debugged, as time-constraints were not allowing for it. This did not affect the experiments of this project, since the measurements were taken in room temperature conditions.

2. EIS Automation

A second Automated Process was developed in the system for enhancing the EIS measurements temporal resolution to approximately 20 minutes (including all I/Q and offset raw-files per frequency) for all 16 frequencies. Once more, the automation handled efficiently any hardware-related errors, and minimized human-induced errors.

3. Partial Automation – for IDAC Stimulation-Current Tuning (per frequency)

The Partial Automation included small automations per control-tab of the GUI. This allowed for faster default configuration setting for any of the Impedance Modalities, while allowing flexibility to the user to adjust some of the commonly altered parameters based on cell-type, or experiment-type. For the IM modality, acquisition of 4096 electrodes for both 1kHz and 10kHz in a 3minutes time-resolution is achieved with the Partial Automation. The increase on the amount of data for the given temporal resolution is significant. For the EIS modality the given flexibility allowed to adjust the current with a fast scan of current-values taking each time into account the electrode-size. When optimized, this feature may be used for effective IDAC tuning (i.e. appropriate stimulation current values).

The last GUI-version with the *Partial Automation* allows higher-density IM measurements for both 1kHz and 10kHz at a great time-resolution. The increase on the amount of data for the given temporal

resolution is significant, even though the file-naming needs to be added manually by the user. The IM Automation requires only the push of one button to obtain all files for both 1kHz and 10kHz, while the EIS Automation uses one button for extracting the chip's offset, and another to obtain both I and Q raw data files over the 16 frequencies. The data-acquisition characteristics did not change for the Automated Processes.

3.1.3 MEA Platforms: Passive HD MEA (Commercial System)

A commercial impedance Analyzer (AutoLab) was used to perform EIS experiments with the same electrode-layout but no active components on-chip. These measurements aimed to validate and that the 1kHz data obtained from the IM measurements are indeed providing information on the sealing-impedance (for cell-adhesion and detachment information). The commercial readout-system is the AutoLab PGSTAT302N (EcoChemie, Netherlands) and was complemented by a sequential multiplexer of 60 electrodes (20 per chip-holder). These were controlled from a digital input/output component (DIO, Agilent u2600 series). The complete setup (Figure 17) was set and explained by Goikoetxea et al. in [52].

Synchronization between the DIO controller and the impedance meter was achieved by a LabView software developed in the past in imec. The stimulation is voltage-based for impedance measurements and the signal is a sinusoid of about 10mV for the spectra of 10Hz to 1MHz. The total number of 17 frequencies, allowed the integer of 1kHz measurements to be included in the frequency sweep.

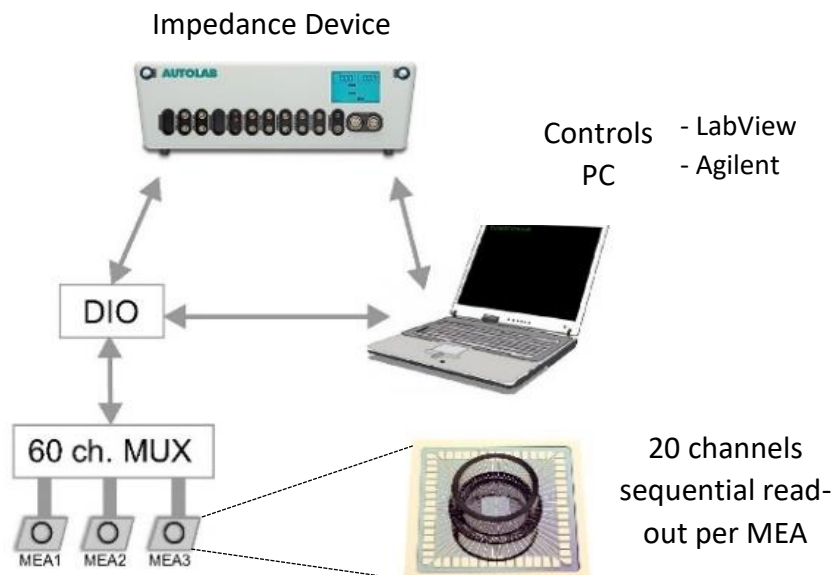


Figure 17. The AutoLab Setup [52].

Due to limited time with the setup, full experimentation was not feasible.

3.2. The Bioassay

3.2.1 Experimental-process: Considerations

Two **types of experiments** were thought to assist in observing efficiently the cell-adhesion/detachment dynamics: *Mid-term* (from cell-suspension until adhesion – 0hrs to ~7hrs), and *Long-term experiments* (from cell-suspension until Day3 – 0hrs to ~60hrs). These can be combined into a single experimental process (*Over-Time Experiments*); i.e. performing measurements of the former and preserving the plated cells in incubation, to continue with the measurements of the next days. The experimental protocol is given in Section 3.2.3.

Potential **key-time-points** and **key-electrode-sizes** should be searched and reported during experimentation and analysis. This means that there may be specific time-dependencies for the experiment to provide fruitful results. For instance, classification between the two cell-lines may be reliable only on the 2nd or the 3rd day and not before; or always during cell-adhesion, for a specific size of the provided electrodes, a cell-line may indicate intense clustering, and nowhere else.

Prior to experimentation, the (cell-free) **cell-medium** is important to be measured, to have a **reference** over which normalization of the absolute data will be feasible if needed. The cell-suspension is another measure to include; however, the variability in cell-size may result in higher-variance over the active MEA area and should be avoided as a reference point. Plating the cells in a **high and low confluency** (i.e. in a high or low density) may provide insight as to how the density of the cell-sample changes behavior.

Calibration for the EIS measurements was not within the time-scope of the project; hence, it is not feasible to derive a single-cell model to fit the data and interpret them. **Basic analytical & statistical methods** to interpret the data are required. Impedance-colormaps per Well for spatial inspection is proposed to generate in order to complement the Box-Plot graph information. Additionally, the lack of EIS information necessitates to use another system to **characterize at least once the MM cell-lines over the spectrum** and see if the IM measurement at 1kHz delivers R_{seal} information for the purposes of this project (e.g. LabView) and validate the assumption that R_{seal} can be measured at 1kHz. An additional **validation tool is confocal microscopy** to see whether the Impedance-Map can infer successfully on cell-positioning.

Proper **Sterilization** of the Experimental Setup and appropriate **chip-and-cell-handling** in the course of an over-time experiment is deemed crucial to ensure that the cell-responses are not affected by malpractice. I.e. chip-packaging and sterilization, cell-imaging protocols, reference-electrode sterility, and appropriate change of medium in fitting time-points. **Enhancing the spatial information** to include all four electrode-measurements per experiment in a real-time response system, suggests that the Partial IM Automation should be used.

3.2.2 Experimental-process: Methods

Due to time restrictions, the stimulation-current calibration for the EIS-Modality of the active MEA could not be finalized, pending now for future work; hence, for the project's completion, only the IM-

modality was used with the Partial-IM-Automation to ensure optimal spatial and temporal resolutions. AutoLab and Confocal Microscopy were used as validation means for system characterization over the spectrum and for validating the optics-free feature of the assay, respectively. Further system-optimizations are required for realizing the MEA's full-potential, yet the results in the experimental process seem promising showing potential (Chapter 4).

Reference Electrodes and Sterility

A *Platinum coil* (*Pt*, *Autolab*) and a *Silver-Silver_Chloride* (*Al-AgCl*, *CMOS-MEA*) external reference (counter) electrode were chosen. A previous comparative study (unpublished) for the MEA systems used in this project showed no significant difference between the two references when used characterized in PBS and melanoma cell-medium. Thus, the results should still be comparable. For this project a small *Petri dish* integrated with a sealed *Al-AgCl* electrode was designed to be used as cell-chamber isolation-cap during experiments; this will be referred from now on as the *ref-cap*. This allowed complete sterility during the over-time IM measurements as well as more stable introduction of the reference electrode to the cell-chamber. The cap was placed on the chip under laminar flow and was removed under laminar flow to sterilize with ethanol 100%. Figure 18 illustrates the *ref-cap*'s architecture and exhibits cells-on chip during experimentation.

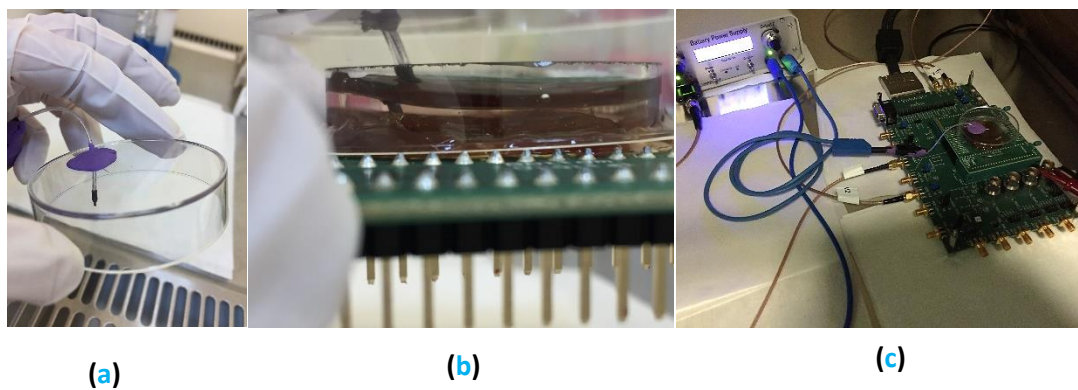


Figure 18. The *ref-cap*: design to use in the experimental setup. (a) The design of the *ref-cap*, (b) when placing it on the chip the reference submerges and stays stable until the experiment is over, (c) application of the *ref-cap* during experimentation.

All experiments were performed in an electrophysiology room, inside a Faradaic cage for *Electromagnetic Interference* (EMI) protection, in a dark-setting (photosensitive materials) at $\sim 23^{\circ}\text{C}$ $\pm 1^{\circ}\text{C}$ (mean \pm SD). The temperature was documented right after a measurement with a room digital thermometer and an infrared hand-thermometer for increased precision close to the chip-cell-chamber. Wells 1-4 of Quadrant 1 were used per experiment for each MEA.

Data Processing, Analysis and Validation

The impedance data were calculated offline in Matlab R2016b (*MathWorks*, USA). The sampled raw-data of the voltage measurements were imported, averaged to obtain a single-value per electrode,

and then they were divided with the magnitude of the stimulation-current (~0.5nA) to attain the absolute impedance value. Further processing included normalization of the values over the gain used by the system and finally, categorization of the data per electrode size, and per well, in an appropriate order and format for generating an Impedance colormap and corresponding graphs. Extra analysis and basic statistics were performed during this project to interpret the results, their significance and their replicability. Figure 19 illustrates the Analysis Process and Figure 20 the Normalization of the Data.

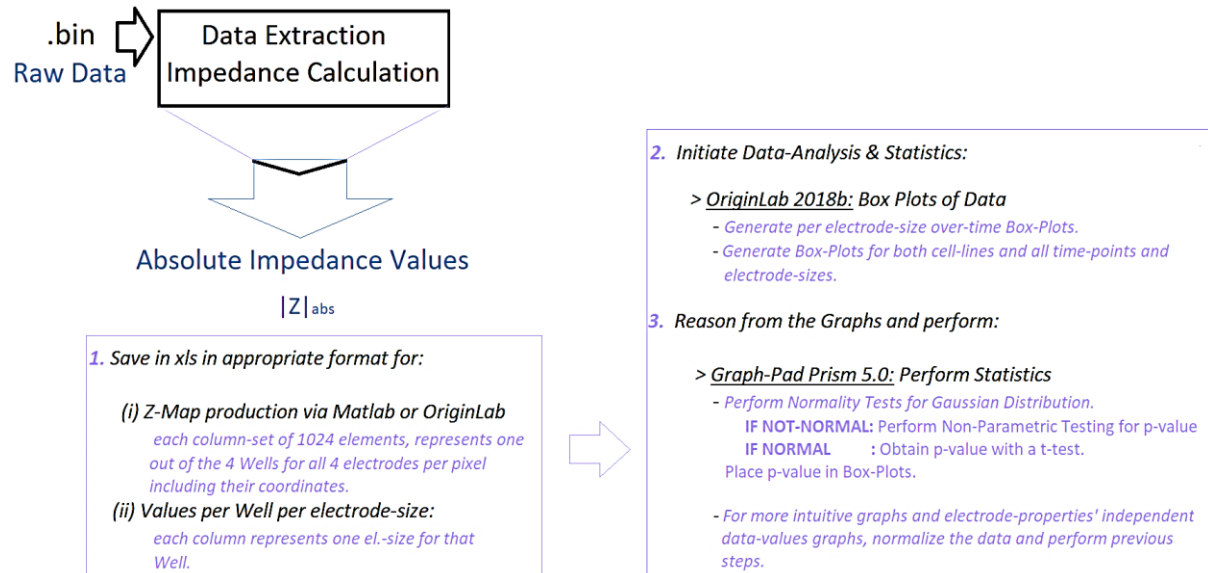


Figure 19. Data Analysis.

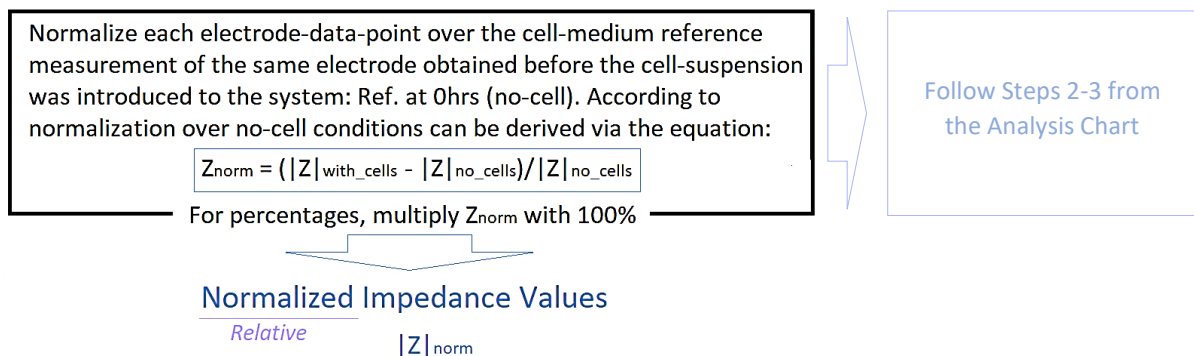


Figure 20. Data Normalization.

In step 3 of the process (figure 19), the normality test is not definitively guiding to non-parametric testing if it is not passed. ANOVA and other statistical methods which assume Gaussian Distribution are robust enough to use despite non-Gaussian behavior of the examined cell-population; that is if the data set is large enough (>100 points based to [54]). Careful thinking is required for the statistical analysis to be chosen eventually. In this project, GraphPad Prism5 was employed for the statistical

testing. Box-Plots and Line-Plots of the measurements were generated with the OriginLab 2017 (Massachusetts, USA) graphing and data analysis software and Excel 2016 (*Microsoft Office*, USA). Data Box-Plots generation, per electrode-size for both cell-lines, absolute Impedance-values Box-Plots' generation, to provide an initial accumulative information on the complete data-set. The Line-Plots are used to depict over time measurement-trends (increase-decrease per time-point) for characteristic electrodes that are indicative of the majority's clustering-behaviors.

MEA Layout Characteristics

The electrodes of the ASIC used in this project are coated with Titanium Nitride (TiN), a known highly-biocompatible material with low-impedance and rough surface (preferred from most cells). Apart from the electrodes, most of the array's surface covered with SiO₂, allowing good cell attachment on the TiN electrode areas. Provided surface topologies (flat or grooved) and TiN-thicknesses (100nm, 300nm or 600nm) were also a few of the considerations of this project. Characterization was performed from fellow researchers and the 600nm TiN with a flat surface was chosen to use in this project.

Confocal Microscopy & Impedance Map for optic-free Assay Validation

For the validation of the results, confocal microscopy was used to compare cell-growth and homogeneity of a cell-population sample on-chip per Well, correlating the image with the corresponding Impedance Colormap (Z-Map) that was created during this project. The cells were visualized on-chip with an LSM 5 Pascal Confocal Zeiss microscope, controlled with the ZEN black software. The objective used was a 10x water-immersion type. For the live-cell staining, calcein-Acetoxyethyl (i.e. calcein-AM) was employed in very low concentrations (~1 μ L aliquoted in 10mL of cell-medium) in the beginning of each to-measure-day. The aliquot was tested before use in the experiments and showed 100% cell-survival in both cell-lines cases, validating the data in the graph of [44].

Chip-preparation for Cell-experiments

Before performing experiments with the ASIC, a certain preparation protocol was normally followed: (i) Wafers were sent for dicing and wirebonding on the carrier-PCBs; (ii) When received back, the chip's active-surface with the exposed wirebonds was inspected under microscope (10x objective), and then a sanity test was performed on the chip to test its electrical characteristics (i.e. initialization, recording, internal offset status); (iii) If everything cleared out, we were applying a biocompatible – when cured – chemical compound that is commonly used in these processes, called *Epoxy* (EPO[®]TECH 353ND-T), in order to package (i.e. cover to insulate and protect) the wirebonds, and the PCB; (iv) The epoxy was also used as a glue to place the glass-ring around the ASIC on the PCB and form the cell-chamber; (v) The chips were then placed in the oven (with extraction) at 120°C for 2 hours to cure the epoxy; (vi) After curing a second sanity test was performed on the chip to document any damage from the described process; (vii) A petri dish is placed to cover and protect the ASIC until it is used in Experiments.

Finishing an experiment: Cells need to be disposed at bio-waste-designated flasks and the chips need to be cleaned both of remaining bio-waste and dirt. For this we used Trypsin for 20 minutes keeping the chip in an incubator. HPW and soap was used to gently-wash the chip. The chip was inspected under microscope and if there was remaining waste, 20 minutes with Targazyme 1% was used.

3.2.3 Proposed Experimental Protocol

The following steps were performed and are proposed:

1. Hydrophilization of the chip-surface by placing for ~15minutes in UVO3 chamber with proper air-extraction (+2minutes minimum extraction time).
2. Sterilization of the MEA and reference electrode under laminar flow: 20minutes fill chamber with Ethanol 100% and next good wash-up with filtered high-purified Water (HPW) and use of a vacuum boy instrument, still under laminar flow. Waiting at least an hour after the UVO3, before commencing any experiments (system was still settling) was necessary.
3. Insertion of MM cell-medium in cell-chamber and placing of the sterile ref-cap on the chip, covering the chamber. Next an IM measurement was performed and the data were stored in .bin-files as references for the particular chip. These references can be used to normalize the absolute impedance data – for shielding parasitic behaviors and focusing only on change-patterns in single-cell Impedance over time.
4. Plating of the Cells-on-chip(s) at 70% (or 10%) confluency on *Day#0*, to perform an IM measurement with the Ref-cap. Documentation of the measurement is given the name *Cell-Suspension at Ohrs*. Cell-lines are plated either on same chip (separated with an insert), or on two separate chips. The former is preferred.
5. Performing an *Over-Hours Experiment* on both cell-lines:
 - a. Repeating the IM measurements for the two cell-lines every 1hour (or every 10-15minutes for enhanced temporal resolution between measurements). In between measurements at least 15minutes of waiting time was kept for the cells to recuperate in the incubator, unless the system is placed inside an incubator and then the IM Automation can perform short time-lapse experimentation (max temporal resolution: 5 minutes between measurements).
 - b. Performing at least 7 measurements with maximum the 1hr interval (cells attach nicely by the 8th hour) and documenting the time of the measurement and temperature.
 - c. Performing quick data extraction and analyzing via box-plots (absolute and normalized data) to observe the changes and decide any separate course of action (i.e. drug-testing, or EIS measurement for certain electrodes).
6. Performing an *Over-Days Experiment* on both cell-lines:
 - a. Repeating the IM measurements twice per day (morning, early evening) for at least 3 days. Usually, interesting time-points were the +15.5hrs and +22.5hrs for Day#1; +35.5hrs and +42hrs for Day#2; and the +53-56hrs for Day#3. Possible extra time-points may be needed for better results.
 - b. Cells need to be kept alive and healthy during this process. Prior to every measurement, a gentle change in the cell-medium helps to dispose any floating dead-cells and debris that will affect the system's conductivity. Chips were kept in the incubator during waiting times.
7. Confocal Images were used for validation. Live-cell-staining with an aliquot of 10mL melanoma cell-medium, 0.1µgr/mL Calcein-AM (non-toxic concentration, used for long-term experiments [44]) will show the alive cells on the chip. One may complement with 10µgr/mL PI dye to stain at the same time dead or dying cells that are still attached.

8. Analyzing the Data with the Matlab Scripts for the IM measurements, and plotting data in Origin with the given templates.
9. Performing necessary normalization over the reference value and statistical testing for the p-value in Graph-Pad Prism and plot again. For performing EIS analysis, a free online EIS Analyzer may to fit the experimental data to the chosen equivalent circuit and validate any important distinct behaviors (this step was not performed in this project).
10. Creating an impedance colormap with Matlab to obtain the cell-localization information (used instead of confocal imaging).
11. Logging any foundlings, data and confocal images.
12. Repeating experimental process multiple times to enhance the findings' statistical significance.
13. Disposing cells and cleaning chips for next plating.

4.

Experimental Process

*"When you have exhausted all possibilities, remember this:
you haven't."*

Thomas Edison

Chapter 4 introduces the promising experimental results and elaborates on them. Per experiment, the main results are separated into two categories: (a) results depicting the classification and (b) results depicting within-heterogeneity for the two cell-lines. A section with the Confocal Images and Impedance colormaps is also presented, to be used as validation for the optics-free capability of the bioassay per experiment. Finally, a brief summary on the findings and the conclusions of this work are given at the end of the Chapter.

4.1. Experimental Report: Findings

The following sub-sections include results and observations that were obtained during the bioassay employment for the MM cell-lines. The diverse experimental processes aimed to address the multidisciplinary demands and concerns of this project (i.e. cell-biology and imaging aspects, biohazardous chemicals' handling, technical troubleshooting and MEA handling, protocol-development and analysis tools).

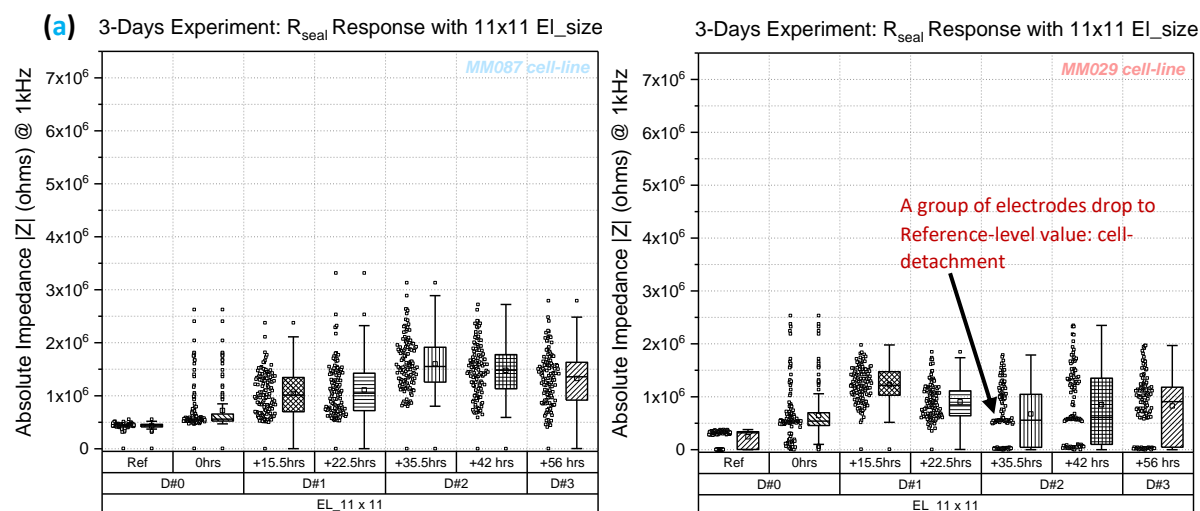
4.1.1 Impedance-based cell response for diverse electrode sizes @ 1kHz

Preliminary experiments were performed to determine electrode size sensitivity to the Melanoma IM responses. A first preliminary experiment was designed to identify electrodes providing the highest variability/heterogeneity indication in response to minor epigenetic changes. This experiment was carried out by recording the single-cell impedance over the course of 3 days, two time per day. Absolute data values (in ohms) for the 1024 readout were obtained and plotted with Box-Plot graphs and scattering data-points in OriginLab, showing responses over time, and per electrode-size (Figure 21(a-d)). The references measurements are compared in Figure 22 to ensure that any cell-based finding is not convoluted by non-cell-system characteristics.

Prior to the morning measurements, the cell medium was gently replenished. Each figure is specific to an electrode size ($11 \times 11 \mu\text{m}^2$, $6.7 \times 7 \mu\text{m}^2$, $4.5 \times 4.5 \mu\text{m}^2$, $2.5 \times 3.5 \mu\text{m}^2$) and cell-type (MM087, MM029). The x-axis is divided in measurement period. This represents the days and hours within the day for each measurement. Per time-point of measurement, the box-plot and on its left the scatter plot is illustrated. The y-axis represents the absolute impedance magnitude ($|Z|$) in ohms.

The following legend will be true for every graph used from now on:

25%~75%
 Median Line
 Mean
 Range within 1.5IQR
 ◊ Outliers



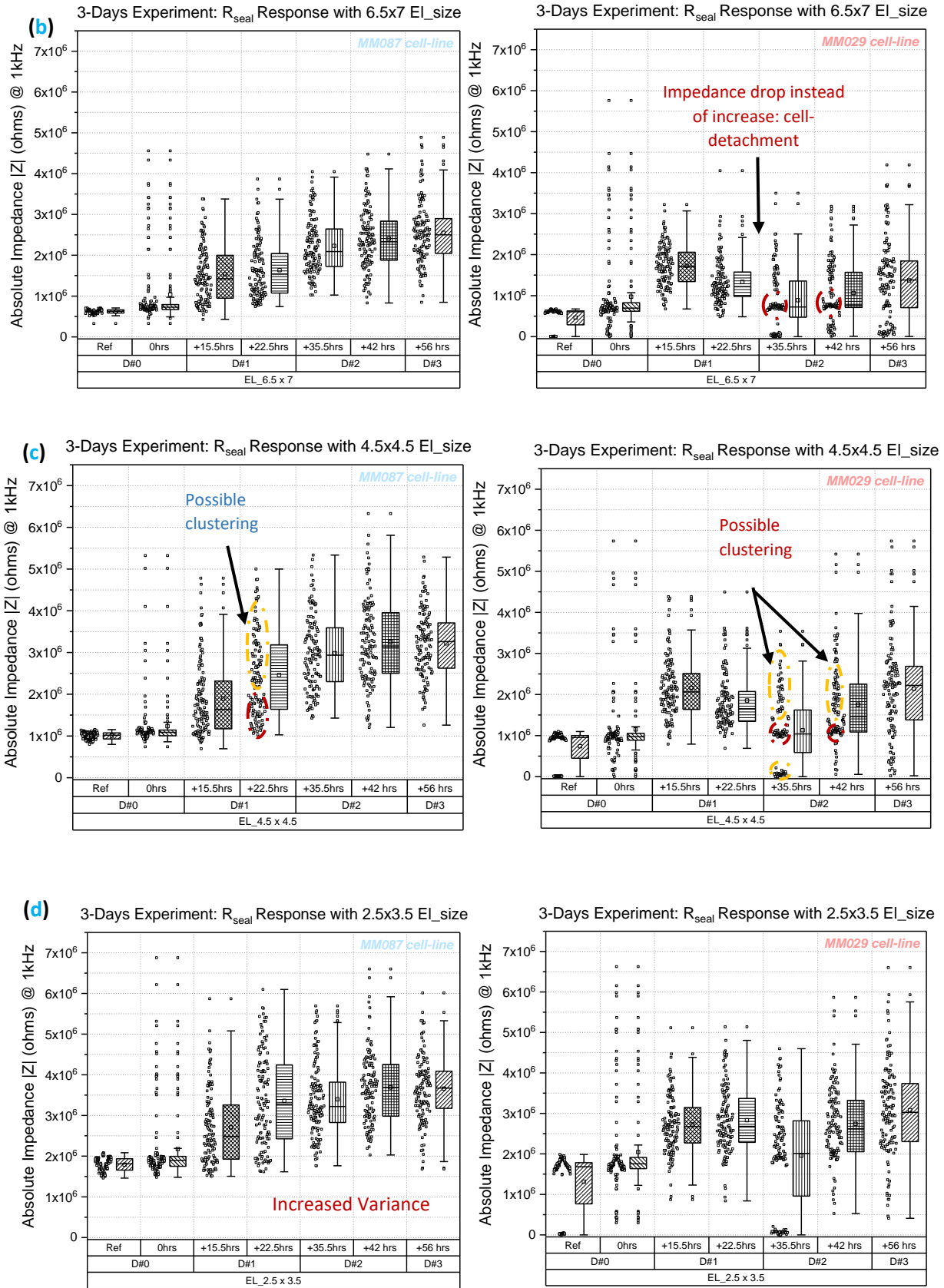


Figure 21. Electrode size-based response of the MM087 & MM029 Cell-Lines in Long-term Experiments. (a) $11 \times 11 \mu\text{m}^2$, (b) $6.5 \times 7 \mu\text{m}^2$, (c) $4.5 \times 4.5 \mu\text{m}^2$, (d) $2.5 \times 3.5 \mu\text{m}^2$

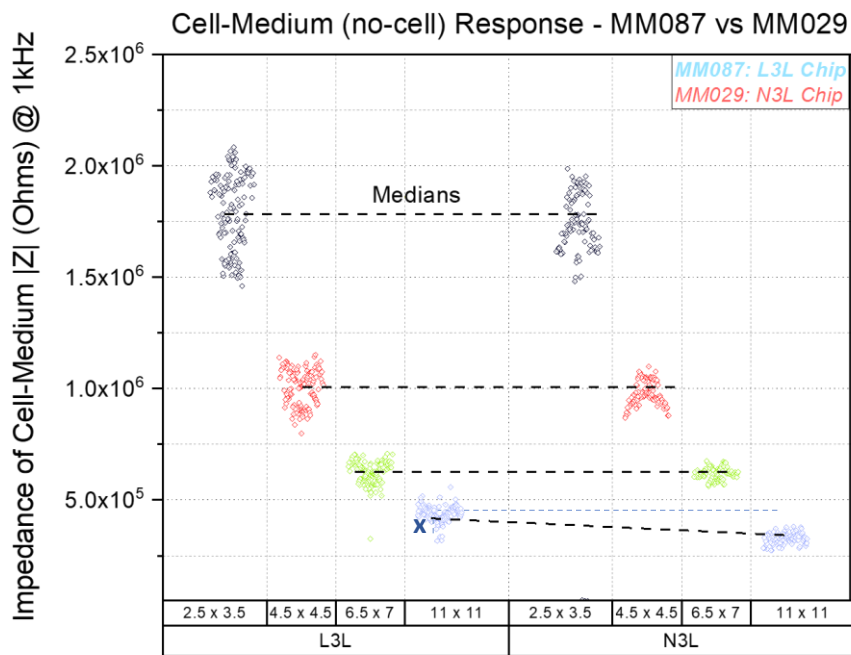


Figure 22. Response of electrodes of different sizes to the MM Cell-Medium in Long-Term Experiments (L3L Chip for MM087, N3L Chip for MM029). This comparison allows the cell-samples to be compared with some reliability so the results are independent of the differences introduced by the system. 11x11 exhibits same difference between the two chip-references; comparison of the MM-lines on this electrode in impedance values would be reliable if their difference is higher than “x” (ohms) depicted in the figure.

The cells were plated in 70% Confluence for both chips. Increased variance in the information was observed in all cases for the smallest electrode-sizes, rendering 2.5x3.5 μm^2 an effective transducer-architecture for both the MM cell-lines. MM029 exhibited a clustering behavior after +22.5hrs, for the 4.5x4.5 μm^2 and 6.5x7 μm^2 electrode sizes. Clustering usually reveals heterogeneous subpopulations within the culture. This however would be erroneous to believe, as there is no spatial-representation of the impedance (i.e. imaging) to verify whether an external factor caused such behavior, or if the electrodes malfunctioned. A good practice would be to check whether some impedances went to cell-medium values. Such a behavior may infer cell-detachment, or cell-motility. If the change affects many electrodes then the latter is less possible, as cells move close to their initial resting area, unless they have detached.

Since confocal imaging was used to validate and point out possible additions that the assay may need to recuperate for the lack of optics, we looked at the confocal pictures to validate. Most cells from the MM029 cell-line were indeed scrapped away from the electrode array of Well #1, by accident, resulting in an impedance drop to cell-medium values (the base). Figure 23 illustrates the cell-growth over time that covered the wiped area within 2 days. The impedance increment can be seen in a 2.5D *Surface Plot* taken with confocal microscopy (*calcein Am aliquot*).

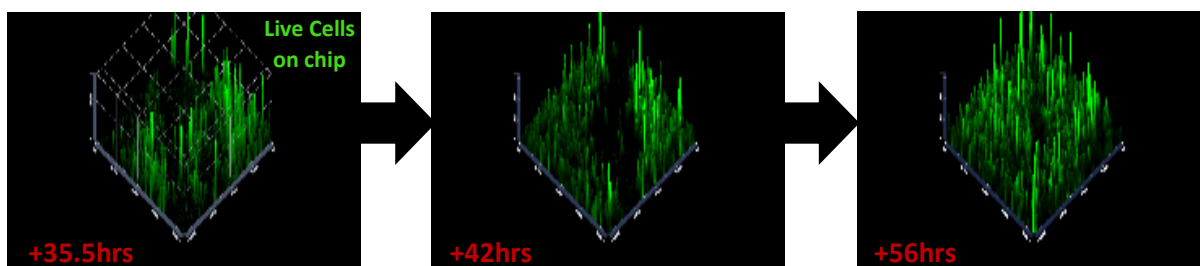


Figure 23. Over-Days IM at 1kHz: MM029 cell-line indicates cell-growth over-days via confocal imaging (2.5D surface).

Figure 23 indicates that on Day #3 the cells were attached reaching the same confluence again as the MM087 cell-line, and thus classification probability may be also valid for that measurement. The graphs are intuitive to a researcher but may lead to fallacies like the given example. For this reason, a way to retrieve the required visual-information of the cell-electrode status during experiments is the Impedance colormaping (Z-Map) and statistics, which quantify the reliability of the measurements. The Z-Map feature is rather successful for the presented experiments as will be seen in section 4.1.3. Main reason is inferred to be the low-electrode-to-electrode pitch ($\sim 15\mu\text{m}$), which is even smaller than the average cell-size (enhanced spatial resolution, high-throughput).

Thus, cell growth and cell motility may be also observed from over-time IM measurements, especially if complemented with time-lapse capabilities. At the same time, such experiments unlock a potential to enhance the information of the observed heterogeneous subpopulations in the spectra, by running an EIS experiment on targeted cells on the MEA. This way, both intracellular and extracellular responses of a distinct signature can be further identified and later classified. No cancer-data have been extracted until now from this modality. As a proof of concept, the spectrum data were obtained by the corresponding passive system (AutoLab), realizing the potential of such a feature.

4.1.2 EIS Information: The spectrum response

Since the phase-data could not be retrieved from the IM modality, a parallel to the active measurements experiment took place to determine whether indeed the R_{seal} was included at 1kHz measurements for the two MM cell-lines and for the employed MEA. Results are noted in Figure 24(a-b).

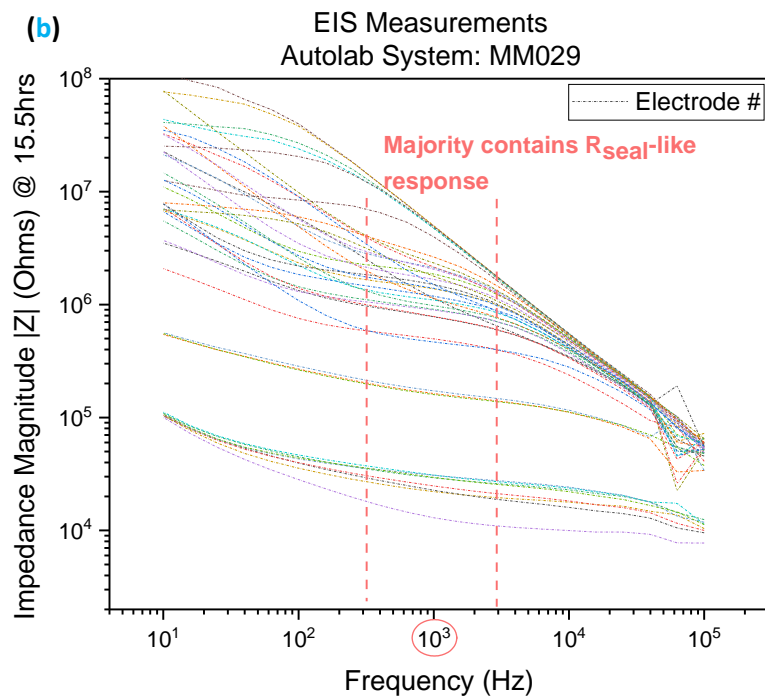
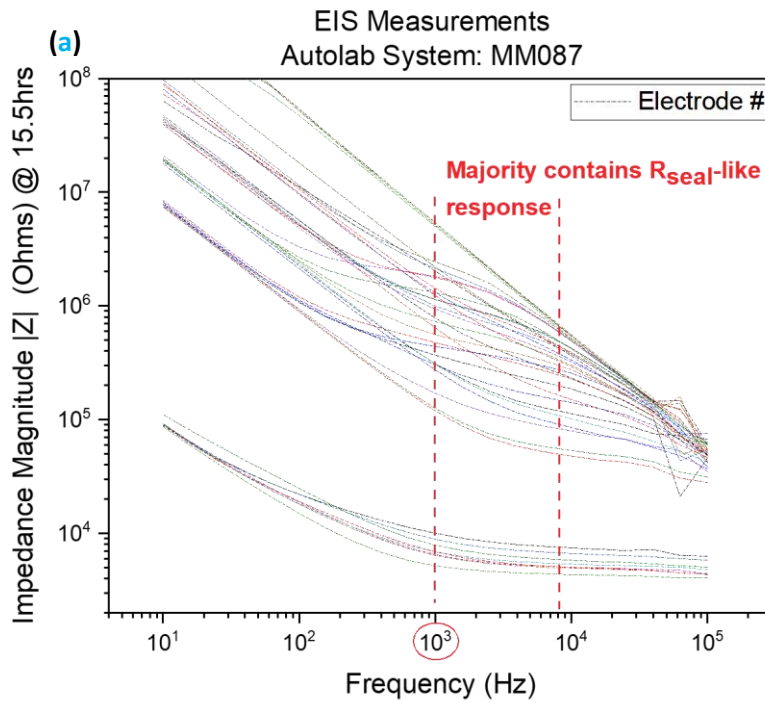


Figure 24 AutoLab measurements to characterize the (a) MM087 and (b) MM029 responses over the spectrum.

When depicted in graphs, R_{seal} is expressed as a *plateau* over a frequency band (no frequency-dependence for R_{seal}). From theory and the above results, it can be inferred that 1kHz lies within range for R_{seal} -characterization of the MM087 cell-line. For MM029, which seems to be in the middle of the plateau for most measurements. EIS characterization with the active-system is deemed important to ensure statistical significance.

4.2 Over-Time IM Measurements: Realizing the Bioassay

Having acquired information of the 1kHz in the spectrum, as well as the processes involved in cells-on-chip experiments, an *Over-Time Experiment* – as suggested in Chapter 3 – was conducted to test the feasibility of the Bioassay and enhance its potential. Along the process, statistics were employed to determine whether the findings could be considered conclusive. However, this was not the case as will be discussed; investing on the analysis and statistical methods behind the assay should be the core of future work.

4.2.1 Experimental Reporting

The process described in 3.2.4 Section of the 3rd Chapter was followed. However, previous experimentation provided enhanced variance conditions when cells detached that created subgroups of potentially-interesting cells. Thus, the 70% confluence was complemented by another chip, seeded at 10% confluence. A total of 4 chips were used in the experiment (two per cell-line, one for each confluence level) to enhance the capacity of the information. Chip-IDs were given to simplify the reporting: Chip 1L (MM087, 70%), chip 2L (MM029, 70%), chip 3L (MM087, 10%), chip 4L (MM029, 10%). The reference (measurements in cell-medium) of each pair and between pairs was associated; basic comparisons can be allowed from chips of the same confluence. Using one of the Automations (Partial Auto) all 4096 electrodes of Quadrant 1 on the chip were measured and saved for offline post processing. The smallest and the biggest sized electrodes are analyzed as their architecture agreed with the MM lines revealing possible heterogeneous responses and propose ways for cell classification.

Both mid-term and long-term experiments were studied. Each measurement and condition, gave information both for Classification and Heterogeneity observations; The former relies on the mean or median difference of the population (average response of the sample) and the latter relies on the clustering patterns within each cell-line. The statistics on the measurements are presented at the end of the long-term experiment.

Log 1

During the mid-term measurements, cell-adhesion from cell-suspension (0hrs) is studied. The entire process lasts approximately ~3-4 hours, keeping 1hr interval in between for 4 chips outside incubator conditions. In this project, an 8-hour process was chosen as the ground-rule for testing, as it is believed to provide further insight in cell-motility dynamics, after adhesion and proliferation initiated. Figure 25(a-b) depicts results from the MM087 and MM029 cell-lines, at 70% and at 10% confluence without any normalization of the extracted data. Figure 26(a-b) depicts the same data-set after normalization over the reference values (no_cell , equation in Figure 20). Electrode sizes 11x11 and 2.5x3.5 were chosen as the most and least variant case respectively to the experimentation.

Main Findings

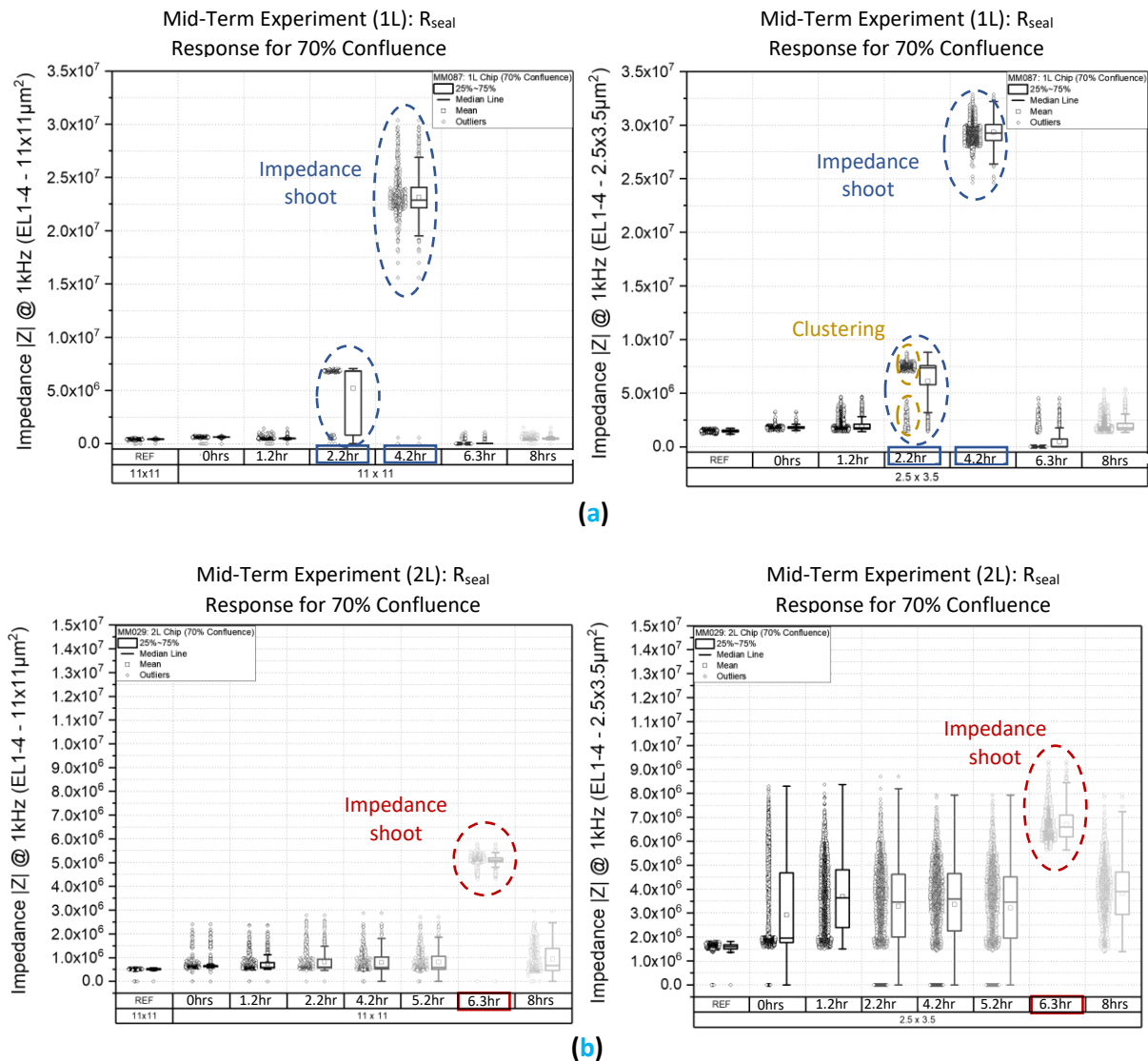


Figure 25. Absolute Impedance Values – Over Time Experiment: Graphs of the two cell-lines (MM029 & MM087 at 70% confluence) showing the adhesion process for largest and smallest electrode-sizes, using impedance (a) MM087-1L and (b) MM029-2L.

Discussion 1A: Classification of MM cell-lines

An abrupt change in Impedance – i.e. Impedance shoot – is noticed for different time-points per cell-line in the system, allowing possibility for classification from the latency of the response in the MM029 cell-line. Many are the considerations a researcher oughts to take into account before concluding to report these results as conclusive. The first one suggests that System Instabilities which intrude to alter the cell-electrode interface response at 1kHz may be the reason behind this response; this comes in line with the time-difference of 3-5 minutes between the two cell-line measurements. A contrary consideration states that the system is not to blame and the intrinsic properties of the cells actually

gave the different response-times due to the cel-lines' increased adhesion dynamics over time. These considerations are recognized; yet no certainty can come from either. For the first, the system is not fully characterized yet (EIS modality is missing) to know what could have cause this. For the second, since the two cell-line were not on the same chip for the measurement, the delay of 3-5 mins between the two lines' measurements could be accounted for the time response variation between the two cell-lines. That is why, more robust ways to use impedance information for classification are given later in the process.

Discussion 2A: Heterogeneity of MM cell-lines

Clustering is observed at +4.2hrs for the MM087 cell-line, an indication of heterogeneity, as the no-cells electrodes are not all having cell-medium responses. Statistically one can infer on the sample after it is observed and recorded multiple times for this cell-line. Continuous real-time measurements would allow to see how the clustering is formed and how it subsides.

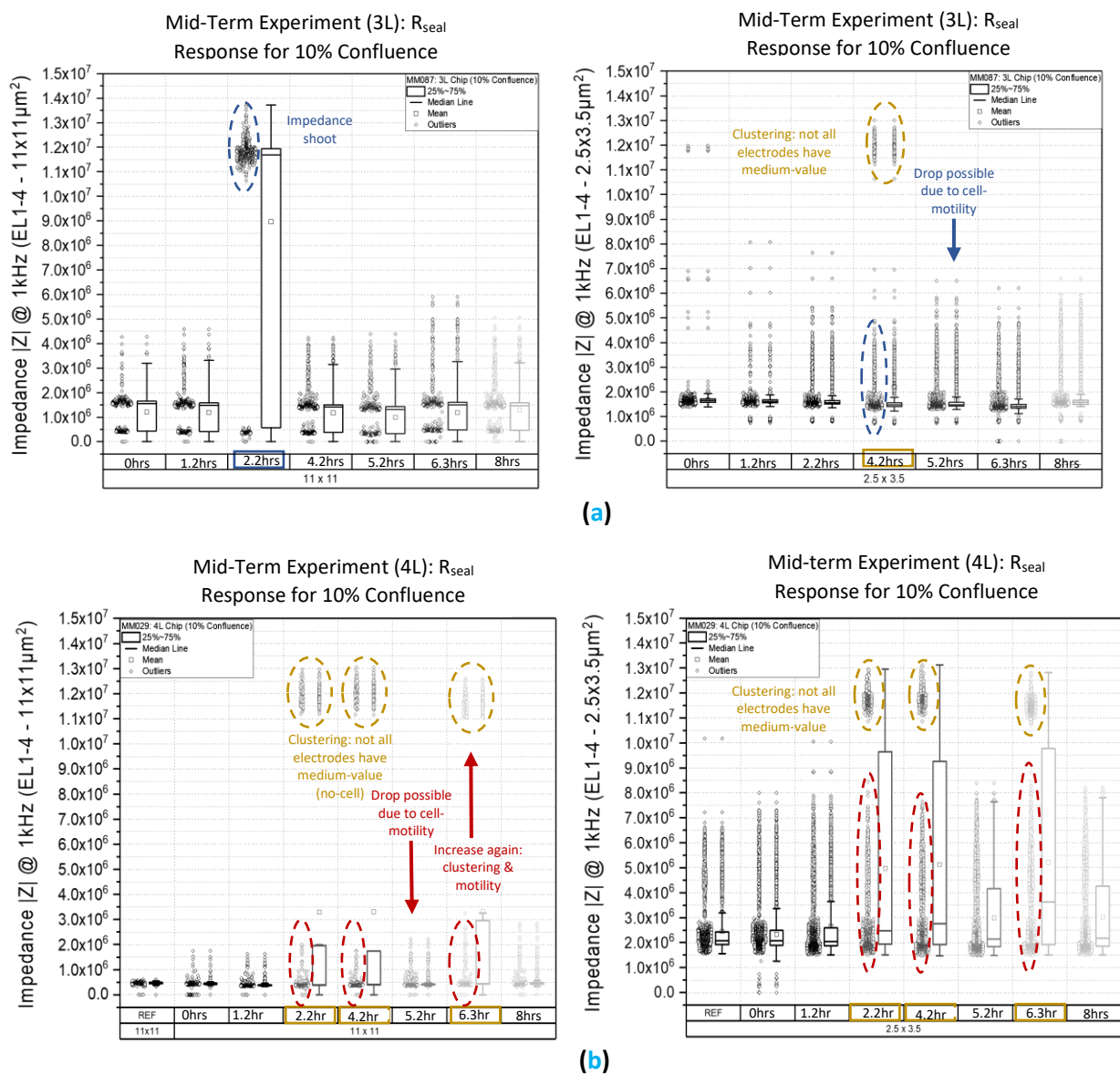


Figure 26. Absolute Impedance Values – Over Time Experiment: Graphs of the two cell-lines (MM029 & MM087 at 10% confluence) showing the adhesion process for largest and smallest electrode-sizes, using impedance (a) MM087-3L and (b) MM029-4L.

Discussion 1B: Heterogeneity of MM cell-lines

An abrupt change of Impedance – i.e. Impedance shoot – is noticed again for the MM087 cell line but not for the MM029. This occurs at the same time-point as the clustering behavior the same cell-line expresses for the smallest electrode size. Can that be a coincidence? Probably not. Either the system is indeed misbehaving, or the cell-population communicates in a way that induces these global yet diverse responses based on the heterogeneity it hosts. Since we do not have the complete system characterized, we cannot trust the individual electrodes' specification-variations for each chip. Normalizing over the cell-medium references would show any constant dependencies that existed and will allow for a clearer comparison, and an intuitive analysis and interpretation of the data. Figures 27(a-b, c-d) and 28(a-b, c-d), contain the *normalized* graphs.

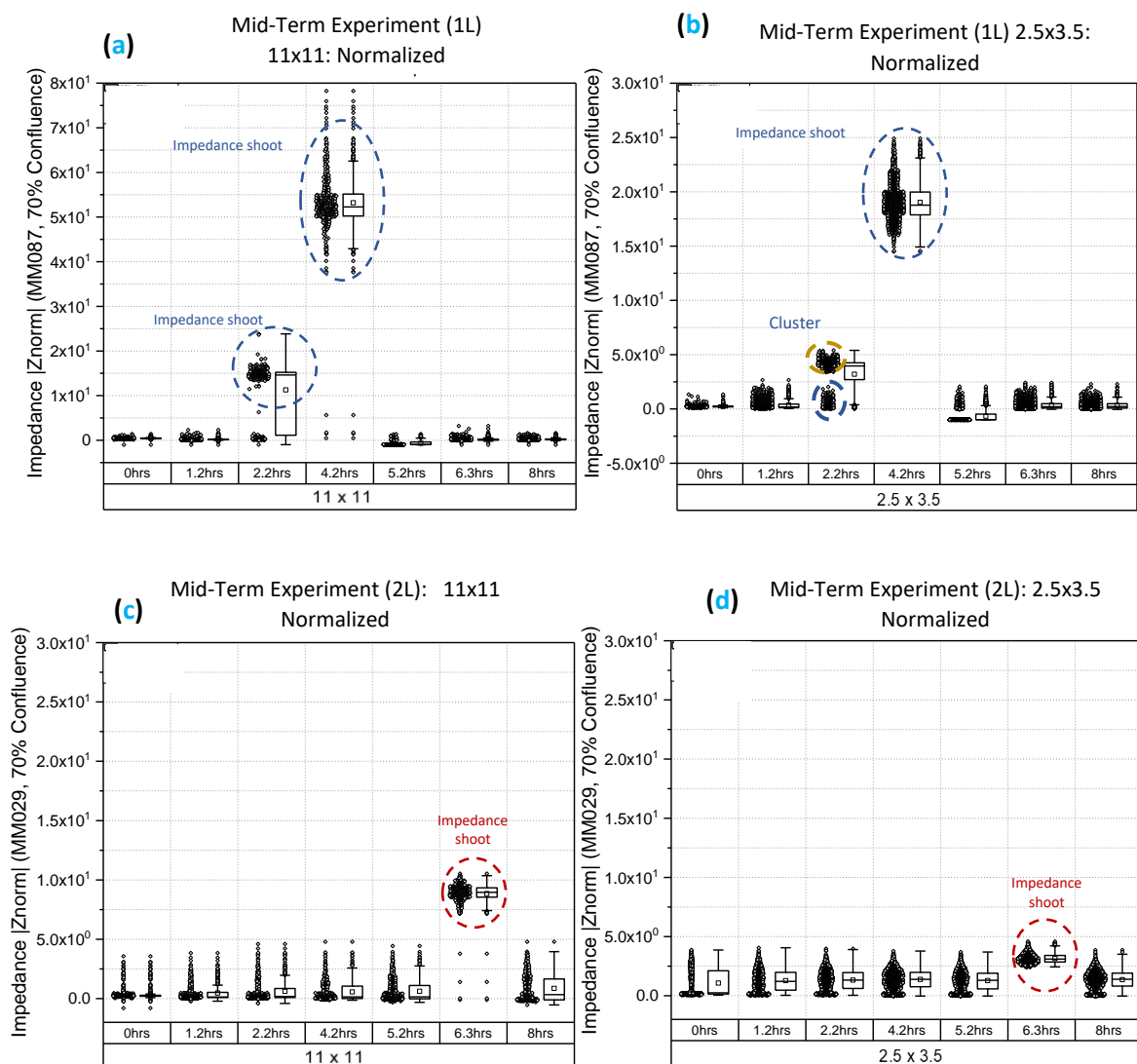


Figure 27. Normalized Impedance Values – Over Time Experiment: Graphs of the two cell-lines (MM029 & MM087 at 70% confluence) showing the adhesion process for largest and smallest electrode-sizes, using impedance (a-b) MM087 and (c-d) MM029.

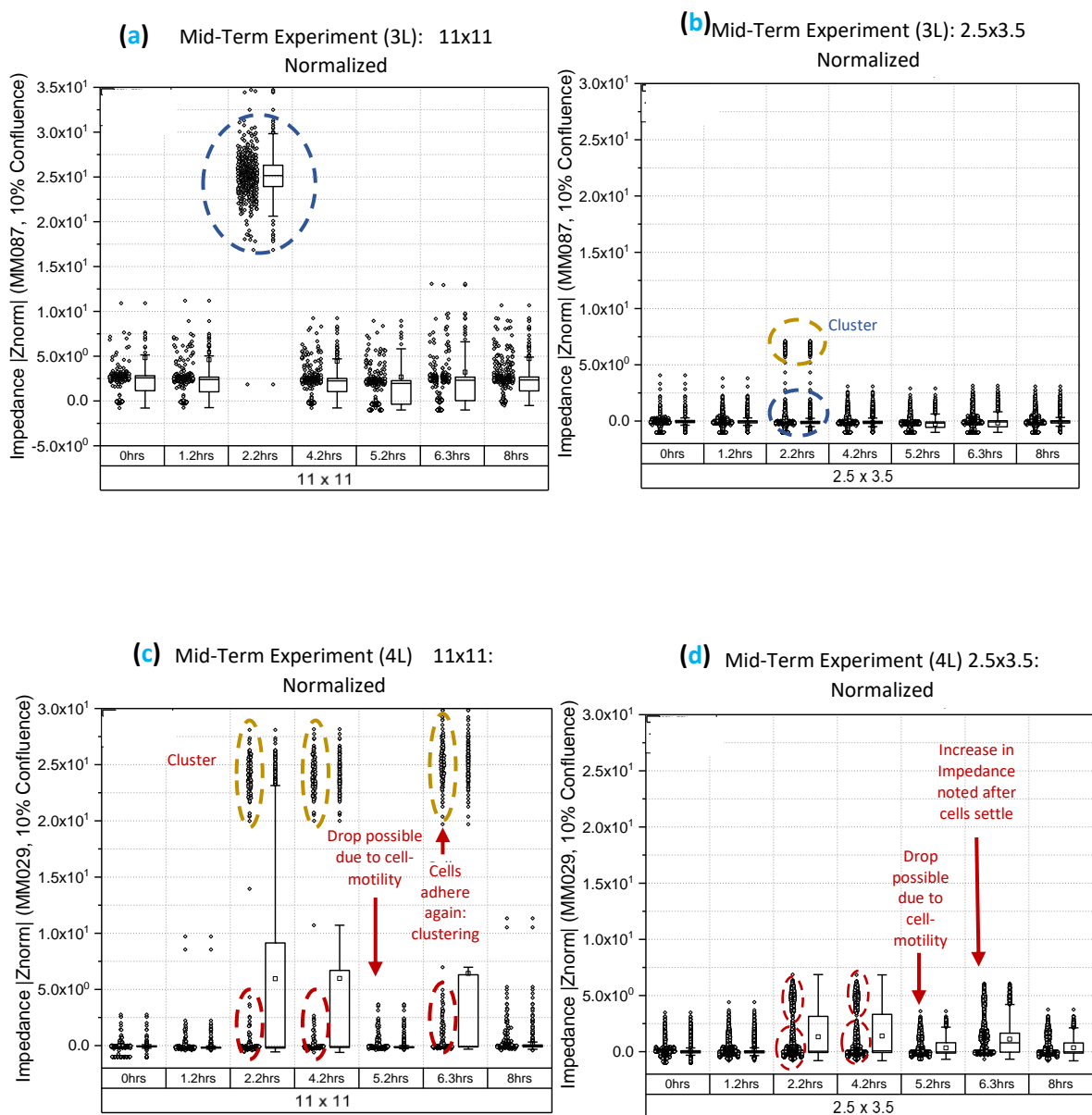


Figure 28. Normalized Impedance Values – Over Time Experiment: Graphs of the two cell-lines (MM029 & MM087 at 10% confluence) showing the adhesion process for largest and smallest electrode-sizes, using impedance (a-b) MM087 and (c-d) MM029.

Discussion 1C: General Conclusion on Heterogeneity and Classification Indications

All in all, the responses of the Impedance shoot did not seem to be a normalization issue; it was still visible in all cases at the corresponding time-points. Notes per cell-line and per confluence (plating) sum up to the following clues of **probable** (still no actual statistics) heterogeneity information:

The MM087 cell-line at 70% Confluence (1L), showed: Impedance-shoot @4.2hrs and Clustering @2.2hrs for both electrode-sizes (Figure31(a) 11X11 μm^2 & Figure31(b) 2.5X3.5 μm^2).

The MM029 cell-line at 70% Confluence (2L), showed: Small Impedance shoot for the smaller electrode size @ 6.3hrs for both electrode-sizes (Figure31(c) 11X11 μm^2 & Figure31(d) 2.5X3.5 μm^2).

The MM087 cell-line at 10% Confluence (3L), showed: Impedance-shoot @6.3hrs Figure32(a) 11X11 μm^2 & Clustering @2.2hrs Figure32(b) 2.5X3.5 μm^2 .

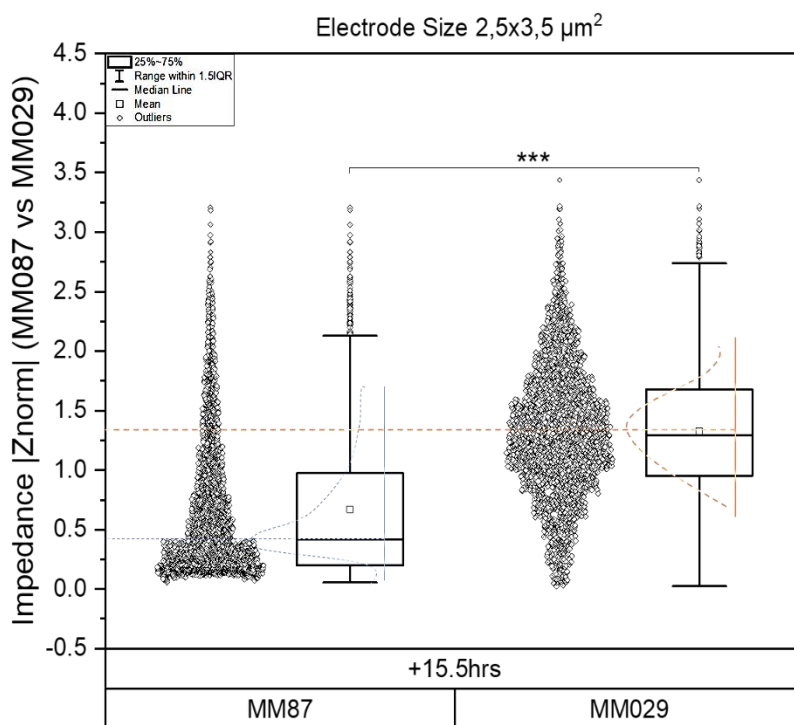
The MM029 cell-line at 10% Confluence (4L), showed: Clustering, i.e. heterogeneity indication for both electrode-sizes (Figure32(c) 11X11 μm^2 & Figure32(d) 2.5X3.5 μm^2) @ 2.2hrs and at 4.2hrs.

The 2.5X3.5 μm^2 electrode size seems to have higher sensitivity in Impedance variations even in the normalized version. This agrees with the preliminary experiments. The following continuum experiment is presented since classification is not deemed appropriate to study in the highly dynamic environment during the cell-adhesion process. Hence, results from the long-term experiment for the 2.5x3.5 electrode size is reported as a proof of concept for the classification technique.

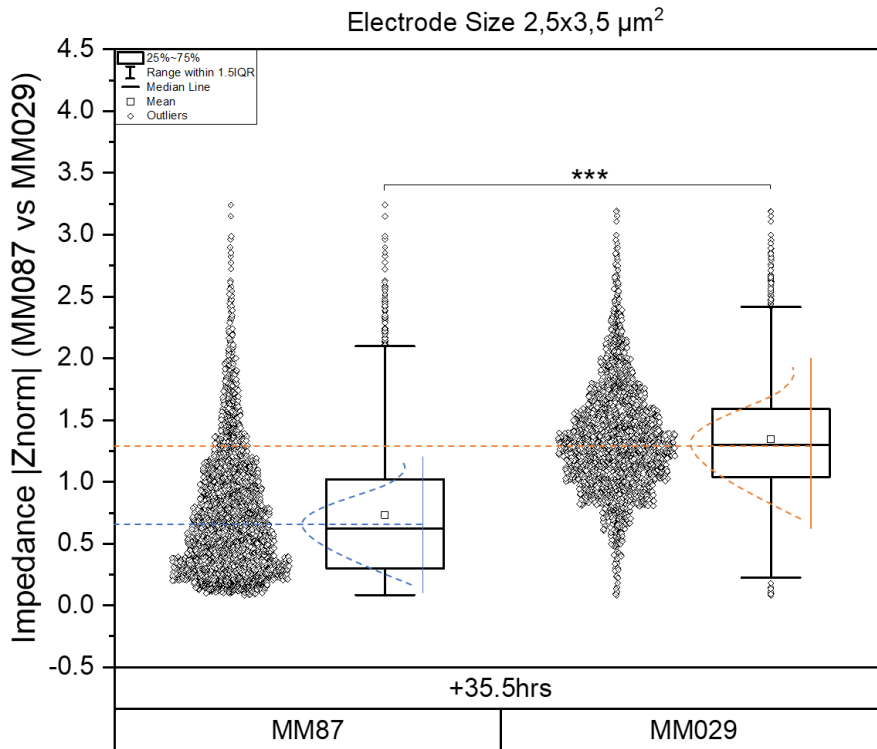
Log 2

To observe in longer time-frames the cell adhesion and detachment dynamics (more natural state), the long-term experimental protocol was initiated. The long-term responses matched the ones of the preliminary experiment. On Day #0 the cell medium was measured to use as a reference and a control for the different chips. The cell-suspension was obtained immediately after cell-seeding, at zero hours. For the next three days, the impedance was obtained once per day. Before every measurement, the cell-medium was being gently replaced with a fresh portion, to eliminate calcein-AM debris that may had been ejected from the cells from the previous day's confocal imaging (affecting the measured values). The 10% confluences provide a rather difficult statistical case, as the cell-growth did not follow normal distribution over time; compared to the 70% confluent chips, 10% confluence provided highly inconclusive results and are not considered here. Figure 29(a-c) shows some indicative data-plots.

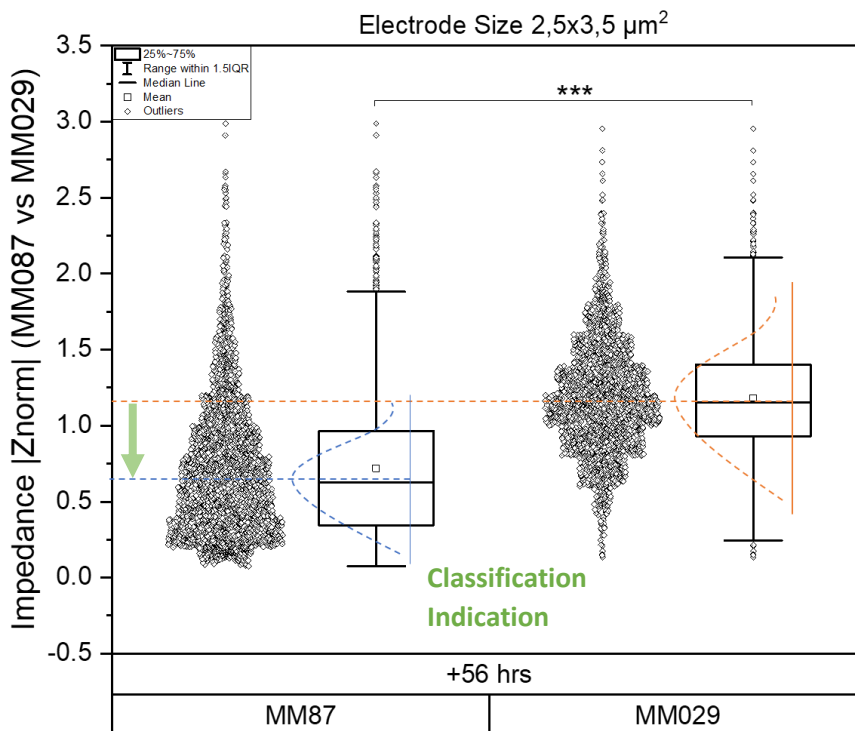
Main Findings



(a)



(b)



(c)

Figure 29. Normalized Impedance Values – mid-term experiment: Graphs of the two cell-lines (MM029 & MM087 at 70% confluence) showing the comparison (i.e. classification indication) between the two cell-lines for the smallest electrode-size, using impedance. The p-value (<0.0001) was obtained by the Kruskal-Wallis non-parametric test (GraphPad Prism5). (a)

Between cell-lines classification is evident for the 70% confluent chip. Basic **statistical analysis** was performed on the data-sets for the overtime experiment to see whether the observed classification – when comparing the two cell-lines – was random or whether it is replicable. This is depicted on the graphs in the form of a p-value obtained after performing a Kruskal-Wallis non-parametric test. The reason of choosing a non-parametric analysis is a two-factor decision: (i) the data-sets failed to pass the commonly used normality tests (i.e. *D'Agostino & Pearson omnibus normality test*) and thus were not following a Gaussian Distribution; and (ii) the extreme variances observed in the box-plots cannot be excluded without biasing the end-results. However, despite the amount of the data, some too high and too low values make it unfeasible to analyze those data with ANOVA. Transformation of the data to logarithms and examining whether they followed a Lognormal Distribution was also executed, giving poor results. Thus, a non-parametric approach, which compares the distribution of the ranks instead, makes the test more robust as the largest value has the largest rank, without mattering how large that is. A small p-value with the Kruskal Test, suggests simply that the distributions of the data-sets (multiple sometimes) are different. The median is normally used to represent an “average” behavior when no-normality can be claimed. Further statistics are needed to verify the observation drawn in Figure 33, for the classification of the two MM cell-lines. For now, these results show potential but remain inconclusive.

Confocal Imaging was performed in the process of the optics-free bioassay validation. It is interesting to see how cells are changing the impedance when they are placed on top of an electrode, and how weird responses may relate to external factors (e.g. wiping of a well) rather than important biological characteristics of the cell-population itself. Below are the confocal imaging pictures showing cell-growth over time Figure 30(a-b) and corresponding confluence of the substrate Figure 30(c).

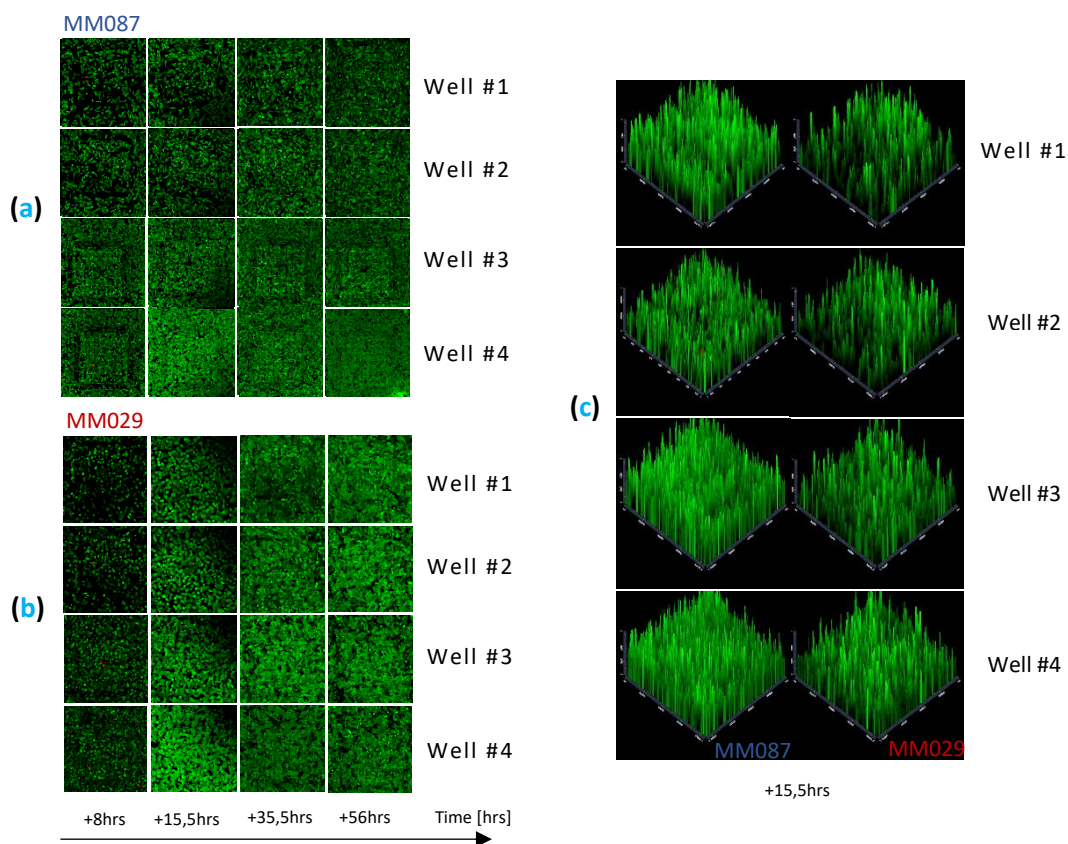


Figure 30. Calcein staining, Confocal Microscopy: Cell-growth over days (a) MM087, 1L (b) MM029, 2L (c) substrate uniformity and cell-coverage for both cell lines, MM087-1L & MM029-2L.

A question rises, as to how one can overcome this lack in information using only the impedance values. As seen in the preliminary experimentation, in some cases it can prove to be misleading if imaging is not used to validate. Below is the proposal of this project to overcome some constraints.

4.2.2 Impedance-Colormap in replacing Confocal Images

Thanks to the high-spatiotemporal resolution the high-throughput and HD MEA provides, Z-Maps at 1kHz will be very indicative of the cell versus no-cell mapping of the active electrode area. In other words, the Impedance-based bioassay is already up to the challenge by presenting a high resolution, optics-free proposal: Impedance Colormap (Z-Map). Proof of this claim is in the next figures Figure 31(a-b). Making the colormap match the actual architecture of each electrode in the well was also tested but it proved less intuitive when illustrating the cell-population spread; thus, it is omitted. The maps are produced per Well number; however, a new matlab-script is under development aiming to create at once all four wells of the Quadrant.

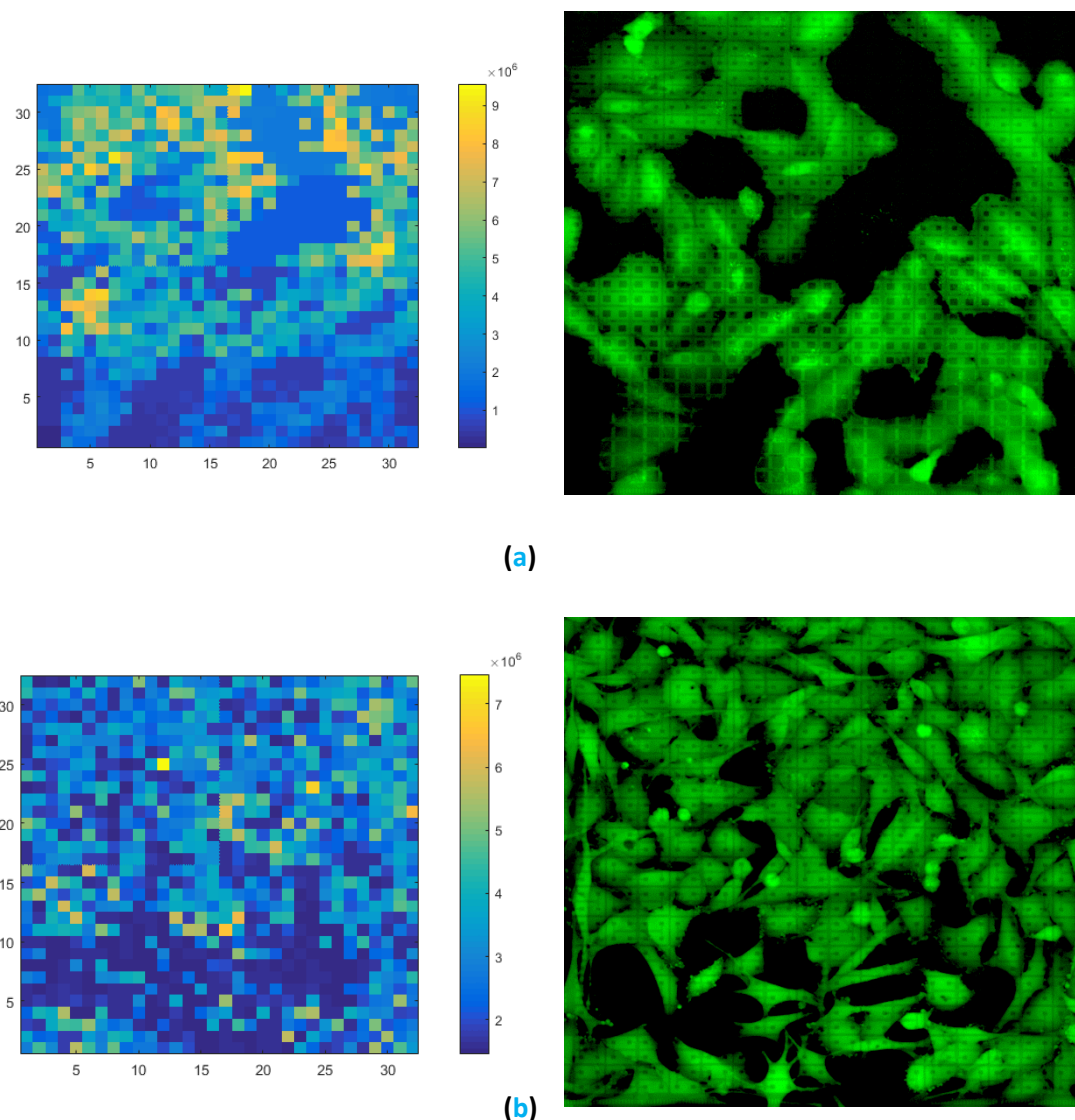


Figure 31. Z-Map – Indicative examples of its potential in replacing the confocal imaging information (a) MM029 (Well1-L4, Day2) and (b) MM087 (Well3-L4, Day3).

Wells 3-4 with the same electrode size everywhere, will show a clearer picture of the population's optical information. This, in accordance with their increased sensitivity in Impedance variance, suggests that these are the ideal wells to work with the bioassay. Techniques to scale up or down the other Wells in parts (i.e. per electrode-size column-set) may be useful to extend the map's capabilities. However, this is not elaborated further in the project, as it serves for future work.

4.2.3 A future analysis-tool to extract classification and heterogeneity information from the Impedance data

While trying to find a way to perform preliminary data analysis in such a big data-set, a concept for studying and maybe identifying heterogeneity was conceived. The final data-matrixes consist of as many rows as the number of electrodes; per electrode, every next-time point of measurement is expressed sequentially in the columns next to it. By plotting 3 or 4 time points in a long-term experiment, certain patterns are derived, based on the increase or decrease in Impedance for every next data point in time. Examples of such "clustering" behavior over-time can be seen in Figure 32.

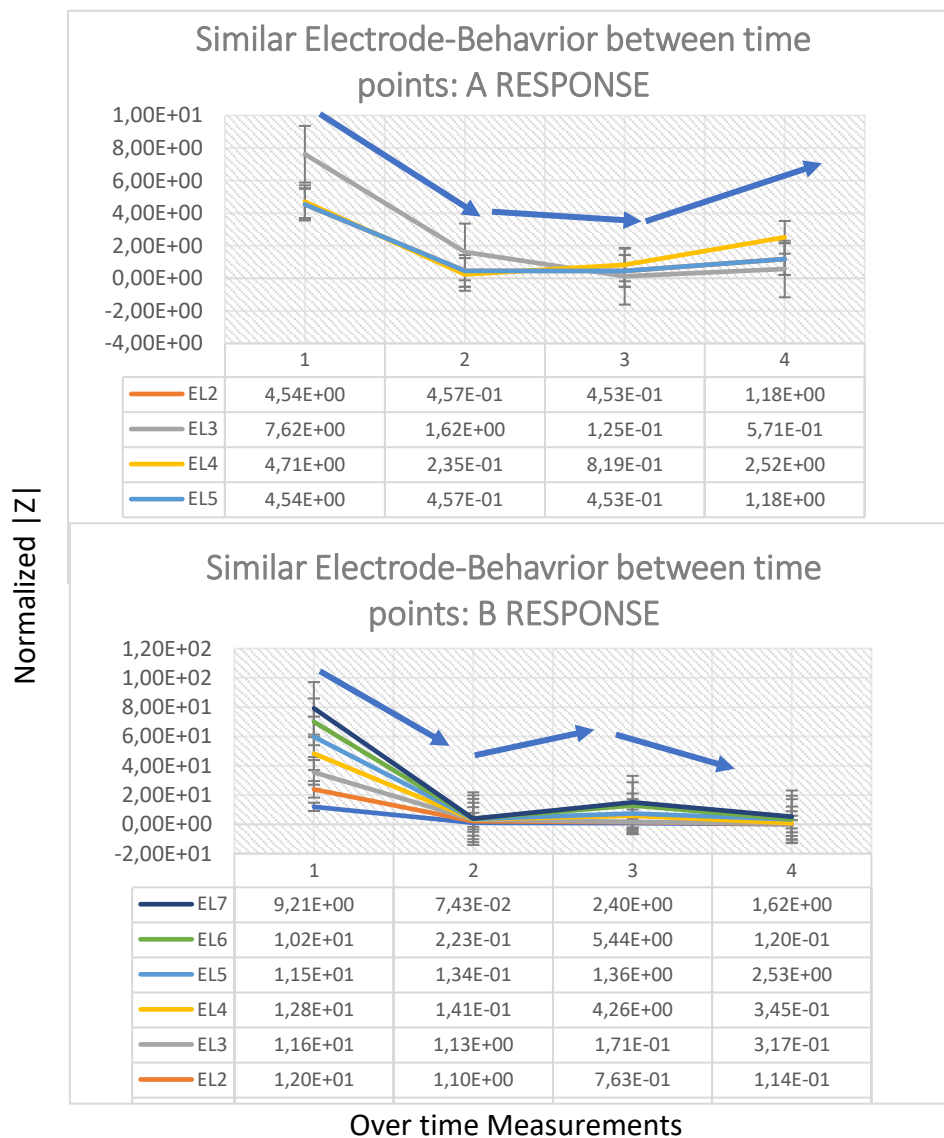


Figure 32. Identification of response patterns for electrodes (i.e. cells) over the time-points of measurements.

Based on this observation, a proposal is made to develop an automated algorithm used to extract all the overtime trends in impedance change (increase/decrease over discrete time) per electrode. An example illustrating the potential of such an algorithm can be seen in the following figure (figure 33):



MM029 > MM087 (~0,5<1 @ +15,5hrs) Not good, too small of a difference
 MM029 < MM087 (~0,7<1 @ +35,5hrs)



MM029 >> MM087 (~1,5>1 @ 56hrs)

Figure 33. Examples of the process to be used to developing a way to detect heterogeneity and achieve classification for MM-cell-lines. A threshold of 1 is set for now (subdue to change with future implementation) to distinguish when a difference is considered adequate and when it does not.

We believe that such patterns over time conceal ways of acquiring and observing heterogeneity for each cell-line, and ultimately between cell-lines. Achieving their identification and classification could provide a great means of identifying abnormal variances over time for certain cells, or minority sub-groups, increasing the efficiency of a targeted cell's specificity-and-testing. In this project, proof of concept behind the idea was managed by manual selection and analysis of the data-sets of the experiment for the smallest electrode size and the 70% confluence populations (figure 33). Of course, the more the time-stamps (i.e. in the long-term experiment a time-stamp is the +15,5hrs, +22hrs, etc) the higher the resolution on the information and consequently, the higher the complexity of the algorithm would rise to be. A trade off would be needed.

Furthermore, by combining the afore mentioned algorithm with the Z-Map information, one can identify the electrodes of "no-cell" status (Z-Map in Matlab allows to obtain the coordinates of the pixel). Then this information may excuse those electrodes from the ongoing analysis, if the cell-information alone is what the researcher looks after. Nonetheless, it would be useful to characterize the electrode response-variations over time with just cell-medium, prior to any cell-studies. This provides the choice to filter in later experimentation the electrode's input (electrodes with cells on top), which may be transient over time and the normalization over the reference did not filter it.

4.3. Summary & Conclusions

In the first two chapters the necessity for a label-free, real-time, and optics-free impedance-based bioassay became evident. MM cancer is a great model to study heterogeneity implications both in diagnosis and in cancer-aggressiveness (i.e. metastatic potential and treatment-resistance). The latest technological achievements in the biosensors' domain allowed the employment of an unprecedented high-throughput MEA prototype, designed by imec, to design an Impedance-based bioassay fit for cancer research, and test experimentally its potential.

The preliminary Impedance-based bioassay was developed experimentally during this project, to assist both MM diagnostics and research on the MM metastatic-potential and treatment-resistance. The main aim of the assay was to investigate the feasibility of using an unprecedented high-throughput CMOS-MEA (developed by imec, 2018) for diverse MM cell-lines' classification and simultaneous within-cell-line clustering indications (i.e. heterogeneity) using over-time IM experiments at 1kHz. Considerations on the processes involved deriving a set of protocols, techniques and control-designs for realizing the end-goal. Control-system IM and EIS Automation designs, sterility protocols, experimental design, statistical analysis procedures for big data-sets, and cell-imaging protocols and tools, are some of the crucial bioassay aspects that this project focused on.

The main proposal presents an over-time experimental protocol of mid-term and long-term experiments, utilizing a high-throughput MEA with increased spatio-temporal resolution (electrode sizes and pitch, parallel readout, Automated processes), for Impedance-based single-cell recordings. IM measurements at 1kHz for two MM cell-lines (MM087 & MM029) showed potential and if complemented with the appropriate statistical and analytical tools, a powerful tool for diagnostics and research in MM cancer – and other types – has been crafted. Electrode-size and normalization techniques were deemed crucial factors that may affect the conclusion over the findings, providing intriguing results in the largest and smallest electrode sizes. A proposal for development a data-analysis tool in the future was presented, stirring the classification and heterogeneity analysis in the direction of over-time changes noticed in each electrode recording; it is an example-based approach to extract the classification and heterogeneity information of normalized IM measurements before, without the end-use of box-plot statistics and graphs.

5.

Discussion & Prospects

*" We keep moving forward, opening new doors, and doing new things,
because we're curious...
...and curiosity keeps leading us down new paths."*

Walt Disney

Chapter 5 is a discussion on the concerns and prospects of the currently proposed bioassay. Promising Analysis-Methodologies are discussed and proposed for future work. After all, this was not the end; only the beginning!

5.1. Discussion

In this paper, an impedance-based bioassay was presented for characterization of the heterogeneity in MM cancer cells and as a possible classification tool between MM cell-lines. Employment of a novel high-density CMOS-MEA system developed by imec, Belgium, allowed for the bioassay-development and testing. Along the way, control system designs of fast and user-friendly Automations for the Impedance measurements were created in LabView to assist the process and make a user-friendly interface. These additions were specifically oriented in the Impedance modalities of the setup. Temporal and spatial resolutions were enhanced, allowing for implementation of an experimental set to test the assay's capabilities and determine any necessary additions for now and the future, in order to make it more robust for research (i.e. Z-Map, templates and scripts for OriginLab and Matlab, statistical methods for validation of findings on the big-data sets, optimizations in the experimental process, etc).

The experimental methods proved the optics-free specification of the assay with the utilization of an Impedance colormap, which was validated by comparing it to confocal images after measurements. However, the biological findings cannot be considered conclusive until a full-scale analysis is conducted on the data. Preliminary results shown a good possibility for classification, while the heterogeneity information cannot be considered conclusive just yet; it requires further experiments in incubator conditions for continuous measurements in real-time, apart from a stronger statistical tool. In such a setup, introducing drug-treatment and keep recording using the fast-response and high-resolution automations for the IM or/and EIS modalities could solidify and arrive to conclusive findings over any response. A novel algorithm proposal to extract all the overtime trends in impedance change (increase/decrease over discrete time) per electrode, has shown promise in classification and heterogeneity information that may be extracted; it is a proposed method for future work, as such patterns we believe that conceal ways of acquiring and observing heterogeneity for each cell-line and ultimately between cell-lines. Proof of concept was managed by manual selection and analysis of a small data-sample, analyzed in the 4th chapter.

Experimentation in triplicate is often used by researchers to prove the results reliability and discard any unknown transient factor that may result in biased results. This is important because like in the example of the *Mid-term* experiment, system Instabilities which intrude to alter the cell-electrode interface response at 1kHz is thought to be the reason behind the observed impedance shoot but we cannot be certain with the provided information. On the same observation, MEA chip used in this project were different per cell-line making it difficult to compare reliably the two cell-lines. To avoid such confusion in the future, we suggest to plate cell-lines on the same MEA chip and separate them with a two-well insert (Figure 34). Wells 1 and 3 have the same electrode configuration as Wells 2 and 4, and a statistically big amount of data per cell-line will still be available per measurement. Often PDMS-based inserts allow for short term experimentation as the material may attract easily contaminants. This is an extra consideration for planning long-term experiments outside an incubator.



Figure 34. Two-well insert

Precursor Drug-Testing experiments with the Bioassay

A precursor cell-experiment presented how *Trypsin* may be used as a positive control for drug-testing the MM cell-lines. The form of the experiment involved visual observation and documentation of the

melanomas adherence, while different concentrations of Trypsin were introduced to cell-samples prepped like Figure 34 (on cover-slips separated with an insert). Such an experiment aimed to decode the MM087 and MM029 cell-lines' behavior in over-time induced cell-death, which involved detachment. The timing in room temperature is very slow, unless 100% of Trypsin is used. Hence, it is proposed to perform a Trypsin-experiment on the cells and observe detachment over time, after inserting the system in incubator conditions, to create a real-time measurement from insertion to population detachment. However, since Trypsin acts faster when heated, a second positive control experiment needs to be conducted before the experimentation with the MEA system.

To conclude, the derived results from the model-bioassay developed in this project seem promising as a first step for shading more light on the initiation of the metastatic cascade in combination to drug-resistivity derived from intense heterogeneities. Further experimentation and development of validation techniques is required.

5.2. Prospects

Observing the experimental results, the developed bioassay is a preliminary version of the one presented in the Methods. Time constraints pushed certain processes out of this thesis' scope. The next step would be to develop further the analytical and statistical methodology of the assay to interpret the data in an unconvoluted and scientifically accepted manner. Incorporation of machine-learning techniques (e.g. the *xCELLigence RTCA HT* by ACEA Biosciences focusing on Impedance signals, or the *Cellprofiler Analyst* proposed by MIT and Harvard for phenotypic classification), would allow for an easier handling and processing of the immense amount of data. In the colormap correlation to the Z-Map section, an idea was presented: techniques to scale up or down Wells 1 and 2 (per electrode-size column-set) may be useful to extend the map's capabilities and should be further investigated. The proposed methodology of analysis in 4.2.2 could be the first place to begin.

Enabling the CMOS-MEA system's capability for EIS measurements (lacking only the stimulation-current calibration after this project) will unlock access to the missing phase information over the spectrum. This would allow a complete characterization of the cell-electrode-electrolyte interface and will be used to extract additional information on single-cells (i.e. electrodes) with a diverse response, filtering-out system-related input; it will be used as an additional interpretation and validation tool. To do so, equivalent circuit models will be developed. Inserting the system into an Incubator and performing the Over-Time Experiments using the IM timelapse-Automation, would extend the assay's specificity to near-physiological measurements, accounting for temperature and CO₂ conditions. Finally, possibilities of utilizing the same bioassay for drug-testing, pursuing to tackle treatment-resistance and to move towards personalized medicine is an equally auspicious prospect. By extracting similar biological information with continuous, real-time responses and by expanding on the current analysis techniques, a multi-purpose bioassay will be established, utilizing impedance data in a large-scale research. Eventually, such a CMOS-MEA may be supplemented with microfluidic systems to create a cancer-on-chip model for even further relevant information on tumor-induced responses and characteristics.

LIST OF ABBREVIATIONS

ALPHABETICALLY ORGANIZED

ADC	: Analog-to-Digital Conversion
Ag-AgCl	: Silver-Silver Chloride
AM	: Aceto-methoxyl
AP	: Action Potential
ASIC	: Application Specific Integrated Circuit
CMOS	: Complementary Metal–Oxide–Semiconductor
CTCs	: Circulating Tumor Cells
CSCs	: Cancer Stem-Cells
DAC	: Digital-to-Analog Converter
DAPI	: Di-Amidino Phenyl-Indole
(E)IS	: (Electrical) Impedance Spectroscopy
EMI	: Electromagnetic Interference
FBS	: Fetal Bovine Serum
GDS	: Graphical Design System (ICs' CAD files)
GUI	: Graphical User Interface
HD	: High Density
HUS	: High-frequency Ultrasound
IARC	: World Health Organization
WHO	: International Agency for Research on Cancer
IC	: Integrated Circuit
LUS	: Low-frequency Ultrasound
IM	: Impedance Monitoring
MEA(s)	: Multi-Electrode Array(s)
MEMS	: Micro-Electro-Mechanical Systems
MM	: Malignant Melanoma
MRI	: Magnetic Resonance Imaging
NCI	: National Cancer Institute
NI	: National Instruments
OCT	: Optical Coherence Tomography
PBS	: Phosphate-Buffered Saline
PCB	: Printed Board Circuit

PET : Positron Emission Tomography
PI : Propidium Iodide
Pt : Platinum
PXI : Peripheral-Component-Interconnect eXtensions for
Instrumentation
RGP Radial-Growth Phase
SU(s) : Stimulation Units
TiN : Titanium Nitride
UART : Universal Asynchronous Receiver/Transmitter
UV : Ultra Violet
VGP : Vertical-Growth Phase
WHO : World Health Organization

APPENDIX

CELL-PASSAGING PROTOCOL

Melanoma Cell-Lines 87 & 29

Cell-Lines:

- (i) An immortalized proliferating melanoma cell-line (M0087).
- (ii) An immortalized metastatic melanoma cell-line (MM029).

Those are both being sub-cultured, while a portion was frozen a week after transfer, for future use and controls' creation.

Split twice per week: Mondays 1:6, and Fridays 1:4 || Cell-lines: MM087 (PROLIFERATING) & MM029 (METASTATIC) || For plating on chip, count cells before plating to control confluency.

Passaging Procedure¹¹:

Materials:

- New Flasks: 25T Flasks.
- Passage under a Laminar-Flow hood, after sterilization.
- For suspending the cells, use Trypsin aliquot of 0.05%. In case there isn't any, mix Trypsin 0.25% from stock with HBSS.
- For Cell-counting: sterilize and use the Cell-Counter Sensor in the cell-suspension.
- Electric Pipette and Pipette tips (all sterilized).
- Fresh Cell-medium (sterilized container).
- Timer.
- Falcon tubes (sterilized).
- Ethanol 70% for the sterilization and lab-tissues.
- Inverted Microscope for Cell-Imaging and Monitoring. An objective of 5X or 10X is good to use.
- Marker.
- Cleaned chips if-needed for cell-plating.

Steps:

1. Check cells in flasks under the microscope. Make sure the cells look healthy and are really confluent.
2. Open intense air for the laminar flow bench.
3. Clean surface in hood.
4. Clean and place inside: necessary materials.
5. TRYPSIN:

¹¹ Acknowledgments to Olga and Bastien who helped me to understand cell-biology and cell-imaging concepts to create and follow this and other cell-processes.

- i) Get trypsin (10mL) falcon tube from the freezer (concentration 0.05).
- ii) Put in Waterbath to warm up.

NOTE: If no ready diluted trypsin, then open the big falcon tubes (concentration 0.25) and make 5 of 10mL aliquots, of 0.05 concentrated trypsin, by diluting the initial with 40mL of HBSS (Ma, and Ca 1X).

6. CELL MEDIUM:

- i) Get Melanoma Cells' Medium from the fridge, clean with 70% Ethanol and place under laminar flow.
- ii) Choose quantity you will need for both the cell-lines:

1:4 --> $(1/4)*5 = 1.25\text{mL}$ of cell-suspension that will enter the new flask. For that you need $10 - 1.25 = 8.75\text{ mL}$ of cell-medium, for the one cell-line, plus the initial 4 mL per flask that will be used to neutralize the Trypsin after cell-detachment. Thus, 25.5 mL are needed for both cell-lines ($12.75\text{mL}*2$), **every Friday**.

1:6 --> $(1/6)*5 = 0.8333\text{mL}$ of cell-suspension that will enter the new flask. For that you need $10 - 0.8333 = 9.2\text{ mL}$ of cell-medium, for the one cell-line, plus the initial 4 mL per flask that will be used to neutralize the Trypsin after cell-detachment. Thus, 26.4 mL are needed for both cell-lines ($13.2\text{mL}*2$), **every Monday**.

- iii) Place in falcon tube and put in Waterbath to warm-up.

6. CELL PASSAGING:

- i) Take out the Trypsin aliquot from the Waterbath, clean and place under laminar flow.
- ii) Bring out of the incubator the first cell-line for splitting, clean and place under laminar flow.
- iii) Remove cell medium from old flask (10mL pipette). Dispose in the designated glass-vile. **!!!CAREFUL NOT TO OVERFLOW PIPETTE!!!**
- iv) Take amount of Trypsin according to Flask-Type you have. For T-25 FLASKS:

You will use 1mL of Trypsin that will be in your cell-suspension in the end per flask. To neutralize its effect, you will add 4mL of cell-medium. In total, your cell-suspension then will be 5 mL for one flask. The final volume needs to be at 10mL. Hence, you will add 5 ml in every new flask.

- (1) 2 mL; Rinse once and dispose trypsin.
- (2) 1 mL; Leave on. Put in incubator and set timer for 2 minutes.

- v) After 2 minutes pass in incubator after the final trypsin injection, take out of the incubator the flask and check under microscope. If cells not fully detached, hit flask to help detachment. Clean flask and bring under laminar flow bench.
- vi) Insert Medium to neutralize the trypsin. For the T-25 FLASK insert 4 mL; --> will create a 5 mL suspension.

The next step depends on what we want to do:

1) Count Cells for cell-platting:

- a) Pipette the cell-suspension a bit up-down in flask.
- b) Take cell suspension and put in falcon tube.
- c) Initiate cell-counter sensor. Insert sensor-tip. Submerge in tube and get:

$lv = [\text{cells}/\text{SuspensionVolume}]$ (i.e. concentration of cells per mL).

Do mathematics to calculate desired volume to place on the chip by knowing the chip area.

$$V \times \text{DesiredVolumeForChip} = \text{CellCountWeWant}$$

- d) Initiate cell-counter sensor. Insert sensor-tip. Submerge in tube and get
- e) Document with the Marker on the Flask
 - i) Cell-line Type and Cell-line ID
 - ii) Splitting Number
 - iii) Date of splitting
 - iv) Splitting ratio and/or cell count
 - v) Name of person responsible
- f) Put New Flask in Incubator.
- g) Dispose single-use materials to the designated areas & clean bench area.

2) No Cell-Count for simple subculturing:

- a) Pipette the cell-suspension a bit up-down in flask.
- b) Take cell suspension and put in new flask directly.
- c) Top-up with medium, to reach: 10 mL (total Volume in 25T flask)
- d) Document with the Marker on the Flask
 - i) Cell-line Type and Cell-line ID
 - ii) Splitting Number
 - iii) Date of splitting
 - iv) Splitting ratio and/or cell count
 - v) Name of person responsible
- e) Put New Flask in Incubator.
- f) Dispose single-use materials to the designated areas & clean bench area.

REFERENCES

- [1] "NCI Dictionary of Cancer Terms", National Cancer Institute, 2017. [Online]. Available: <https://www.cancer.gov/publications/dictionaries/cancer-terms?search=cancer>. [Accessed: 20-Nov- 2017].
- [2] "WHO Cancer Control Programme", *World Health Organization*, 2017. [Online]. Available: <http://www.who.int/cancer/en/>. [Accessed: 20-Nov- 2017].
- [3] E. Lee, H. Song and C. Chen, "Biomimetic on-a-chip platforms for studying cancer metastasis", *Current Opinion in Chemical Engineering*, vol. 11, pp. 20-27, 2016.
- [4] D. Rigel, J. Russak and R. Friedman, "The Evolution of Melanoma Diagnosis: 25 Years Beyond the ABCDs", *CA: A Cancer Journal for Clinicians*, vol. 60, no. 5, pp. 301-316, 2010.
- [5] U. Litzenburger, J. Buenrostro, B. Wu, Y. Shen, N. Sheffield, A. Kathiria, W. Greenleaf and H. Chang, "Single-cell epigenomic variability reveals functional cancer heterogeneity", *Genome Biology*, vol. 18, no. 1, 2017.
- [6] H. Khalil, M. Heulot and D. Barras, "Peptides and biocomplexes in anticancer therapy", *Physical Sciences Reviews*, vol. 1, no. 6, 2016.
- [7] M. Tellez-Gabriel, B. Ory, F. Lamoureux, M. Heymann and D. Heymann, "Tumour Heterogeneity: The Key Advantages of Single-Cell Analysis", *International Journal of Molecular Sciences*, vol. 17, no. 12, p. 2142, 2016.
- [8] G. Lee and R. R Hall, "Cancer Stem Cells: Cellular Plasticity, Niche, and its Clinical Relevance", *Journal of Stem Cell Research & Therapy*, vol. 06, no. 10, 2016.
- [9] "OpenStax CNX", *Cnx.org*, 2017. [Online]. Available: <http://cnx.org/contents/14fb4ad7-39a1-4eee-ab6e-3ef2482e3e22@8.24>. [Accessed: 20-Nov- 2017].
- [10] Blausen.com staff (2014). "Medical gallery of Blausen Medical 2014". *WikiJournal of Medicine* 1 (2). DOI:10.15347/wjm/2014.010. ISSN 2002-4436.
- [11] J. Ross and E. Slodkowska, "Circulating and Disseminated Tumor Cells in the Management of Breast Cancer", *American Journal of Clinical Pathology*, vol. 132, no. 2, pp. 237-245, 2009.
- [12] B. Shannan, M. Perego, R. Somasundaram and M. Herlyn, "Heterogeneity in Melanoma", *Melanoma*, pp. 1-15, 2015.
- [13] M. Boone, S. Norrenberg, G. Jemec and V. Del Marmol, "High-definition optical coherence tomography imaging of melanocytic lesions: a pilot study", *Archives of Dermatological Research*, vol. 306, no. 1, pp. 11-26, 2013.
- [14] J. PATEL, S. KONDA, O. PEREZ, S. AMINI, G. ELGART and B. BERMAN, "Newer technologies/techniques and tools in the diagnosis of melanoma", *Eur. J. Dermatology*, vol. 18, no. 6, pp. 617-631, 2008.

- [15] L. Ferris and R. Harris, "New Diagnostic Aids for Melanoma", *Dermatologic Clinics*, vol. 30, no. 3, pp. 535-545, 2012.
- [16] X. Zhao, H. Zhuang, S. Yoon, Y. Dong, W. Wang and W. Zhao, "Electrical Impedance Spectroscopy for Quality Assessment of Meat and Fish: A Review on Basic Principles, Measurement Methods, and Recent Advances", *Journal of Food Quality*, vol. 2017, pp. 1-16, 2017.
- [17] D. Dean, T. Ramanathan, D. Machado and R. Sundararajan, "Electrical impedance spectroscopy study of biological tissues", *Journal of Electrostatics*, vol. 66, no. 3-4, pp. 165-177, 2008.
- [18] R. Braun, J. Mangana, S. Goldinger, L. French, R. Dummer and A. Marghoob, "Electrical Impedance Spectroscopy in Skin Cancer Diagnosis", *Dermatologic Clinics*, vol. 35, no. 4, pp. 489-493, 2017.
- [19] A. Han, L. Yang and A. Frazier, "Quantification of the Heterogeneity in Breast Cancer Cell Lines Using Whole-Cell Impedance Spectroscopy", *Clinical Cancer Research*, vol. 13, no. 1, pp. 139-143, 2007.
- [20] Y. Xu, X. Xie, Y. Duan, L. Wang, Z. Cheng and J. Cheng, "A review of impedance measurements of whole cells", *Biosensors and Bioelectronics*, vol. 77, pp. 824-836, 2016.
- [21] L. Arias, C. Perry and L. Yang, "Real-time electrical impedance detection of cellular activities of oral cancer cells", *Biosensors and Bioelectronics*, vol. 25, no. 10, pp. 2225-2231, 2010
- [22] S. Tsai and M. Wang, "24 h observation of a single HeLa cell by impedance measurement and numerical modeling", *Sensors and Actuators B: Chemical*, vol. 229, pp. 225-231, 2016
- [23] P. Åberg, U. Birgersson, P. Elsner, P. Mohr and S. Ollmar, "Electrical impedance spectroscopy and the diagnostic accuracy for malignant melanoma", *Experimental Dermatology*, vol. 20, no. 8, pp. 648-652, 2011
- [24] P. Wang and Q. Liu, *Cell-based biosensors*. Boston: Artech House, 2010, pp. 37-64
- [25] "THE EIS TECHNOLOGY", *Scibase*, 2017. [Online]. Available: <https://scibase.com/en/the-eis-technology/>. [Accessed: 27-Nov- 2017].
- [26] *Rockland-inc.com*, 2018. [Online]. Available: <https://rockland-inc.com/patient-derived-tumor-models.aspx>. [Accessed: 25- Jun- 2018].
- [27] D. Ren and C. Chui, "Feasibility of Tracking Multiple Single-Cell Properties with Impedance Spectroscopy", *ACS Sensors*, vol. 3, no. 5, pp. 1005-1015, 2018.
- [28] "THE EIS TECHNOLOGY", patented by the Karolinska Institute of Stockholm, Scibase, 2018. [Online]. Available: <https://scibase.com/the-eis-technology/>. [Accessed: 25- Jun- 2018].
- [29] J. Malvey, A. Hauschild, C. Curiel-Lewandrowski, P. Mohr, R. Hofmann-Wellenhof, R. Motley, C. Berking, D. Grossman, J. Paoli, C. Loquai, J. Olah, U. Reinhold, H. Wenger, T. Dirschka, S. Davis, C. Henderson, H. Rabinovitz, J. Welzel, D. Schadendorf and U. Birgersson, "Clinical performance of the Nevisense system in cutaneous melanoma detection: an international, multicentre, prospective and blinded clinical trial on efficacy and safety", *British Journal of Dermatology*, vol. 171, no. 5, pp. 1099-1107, 2014.

- [30] H. Ceder, A. Sjöholm Hylen, A. Wennberg Larko and J. Paoli, "Evaluation of electrical impedance spectroscopy as an adjunct to dermoscopy in short-term monitoring of atypical melanocytic lesions", *Dermatology Practical & Conceptual*, vol. 6, no. 4, 2016.
- [31] C. Lopez, H. Chun, L. Berti, S. Wang, J. Putzeys, C. Van Den Bulcke, J. Weijers, A. Firrincieli, V. Reumers, D. Braeken and N. Van Helleputte, "A 16384-electrode 1024-channel multimodal CMOS MEA for high-throughput intracellular action potential measurements and impedance spectroscopy in drug-screening applications", *2018 IEEE International Solid - State Circuits Conference - (ISSCC)*, 2018.
- [32] J. Dragas, V. Viswam, A. Shadmani, Y. Chen, R. Bounik, A. Stettler, M. Radivojevic, S. Geissler, M. Obien, J. Muller and A. Hierlemann, *In Vitro Multi-Functional Microelectrode Array Featuring 59 760 Electrodes, 2048 Electrophysiology Channels, Stimulation, Impedance Measurement, and Neurotransmitter Detection Channels*, *IEEE Journal of Solid-State Circuits*, vol. 52, no. 6, pp. 1576-1590, 2017.
- [33] J. Park, T. Chi, A. Su, Chengjie Zhu, Jung Hoon Sung, Hee Cheol Cho, M. Styczynski and Hua Wang, "A high-density CMOS multi-modality joint sensor/stimulator array with 1024 pixels for holistic real-time cellular characterization", *2016 IEEE Symposium on VLSI Circuits (VLSI-Circuits)*, 2016.
- [34] D. Borkholder, "Cell Biosensors Using Microelectrodes", PhD Dissertation, Stanford University, 1998.
- [35] A. Hierlemann, O. Brand, C. Hagleitner and H. Baltes, "Microfabrication techniques for chemical/biosensors", *Proceedings of the IEEE*, vol. 91, no. 6, pp. 839-863, 2003.
- [36] M. Obien, K. Deligkaris, T. Bullmann, D. Bakkum and U. Frey, "Revealing neuronal function through microelectrode array recordings", *Frontiers in Neuroscience*, vol. 8, 2015.
- [37] M. Medeiros, A. Mestre, P. Inácio, J. Santos, I. Araujo, J. Bragança, F. Biscarini and H. Gomes, "Performance assessment of polymer based electrodes for in vitro electrophysiological sensing: the role of the electrode impedance", *Organic Sensors and Bioelectronics IX*, 2016.
- [38] E. Barsoukov and J. Macdonald, *Impedance spectroscopy*. Hoboken, N.J.: Wiley-Interscience, 2005.
- [39] J. Macdonald, "Impedance Spectroscopy", *Annals of Biomedical Engineering*, vol. 20, pp. 289-305, 1992.
- [40] R. Pradhan, A. Mitra and S. Das, "Characterization of electrode/electrolyte interface for bioimpedance study", *IEEE Technology Students' Symposium*, 2011.
- [41] E. McAdams, A. Lackermeier, J. McLaughlin, D. Macken and J. Jossinet, "The linear and non-linear electrical properties of the electrode-electrolyte interface", *Biosensors and Bioelectronics*, vol. 10, no. 1-2, pp. 67-74, 1995.
- [42] P. Massobrio, G. Massobrio and S. Martinoia, "Interfacing Cultured Neurons to Microtransducers Arrays: A Review of the Neuro-Electronic Junction Models", *Frontiers in Neuroscience*, vol. 10, 2016.
- [43] Verfaillie, A. et al. *Decoding the regulatory landscape of melanoma reveals TEADS as regulators of the invasive cell state*. *Nat. Commun.* 6:6683 doi: 10.1038/ncomms7683 (2015).
- [44] B. Jonsson, G. Liminga, K. Csoka, H. Fridborg, S. Dhar, P. Nygren and R. Larsson, "Cytotoxic activity of calcein acetoxymethyl ester b(calcein/AM) on primary cultures of human

- haematological and solid tumours", *European Journal of Cancer*, vol. 32, no. 5, pp. 883-887, 1996.
- [45] A. Ray and J. Weiland, "Structures, Materials, and Processes at the Electrode-to-Tissue Interface", *Visual Prosthetics*, pp. 113-135, 2011.
- [46] W. Franks, I. Schenker, P. Schmutz and A. Hierlemann, "Impedance Characterization and Modeling of Electrodes for Biomedical Applications", *IEEE Transactions on Biomedical Engineering*, vol. 52, no. 7, pp. 1295-1302, 2005.
- [47] E. Pasqualotto, A. Ferrario, M. Scaramuzza, A. De Toni and M. Maschietto, "Monitoring Electropermeabilization of Adherent Mammalian Cells Through Electrochemical Impedance Spectroscopy", *Procedia Chemistry*, vol. 6, pp. 79-88, 2012.
- [48] M. Spira and A. Hai, "Multi-electrode array technologies for neuroscience and cardiology", *Nature Nanotechnology*, vol. 8, no. 2, pp. 83-94, 2013.
- [49] L. Arias, C. Perry and L. Yang, "Real-time electrical impedance detection of cellular activities of oral cancer cells", *Biosensors and Bioelectronics*, vol. 25, no. 10, pp. 2225-2231, 2010.
- [50] H. Jahnke, A. Heimann, R. Azendorf, K. Mpoukouvalas, O. Kempfski, A. Robitzki and P. Charalampaki, "Impedance spectroscopy—An outstanding method for label-free and real-time discrimination between brain and tumor tissue in vivo", *Biosensors and Bioelectronics*, vol. 46, pp. 8-14, 2013.
- [51] P. Chao, E. Huang, K. Cheng and Y. Huang, "Electrical Impedance Spectroscopy as Electrical Biopsy for Monitoring Radiation Sequelae of Intestine in Rats", *BioMed Research International*, vol. 2013, pp. 1-7, 2013.
- [52] E. Goikoetxea, D. Routkevitch, A. de Weerd, J. Green, H. Steenackers and D. Braeken, "Impedimetric fingerprinting and structural analysis of isogenic E. coli biofilms using multielectrode arrays", *Sensors and Actuators B: Chemical*, vol. 263, pp. 319-326, 2018.
- [53] Y. Hong, Y. Wang, W. Goh, Y. Gao and L. Yao, "Analysis of monolithic I/Q based impedance measurement circuits: Impact of non-ideal circuit effects on accuracies", *2016 International Symposium on Integrated Circuits (ISIC)*, 2016.
- [54] "GraphPad Statistics Guide", *Graphpad.com*, 2018. [Online]. Available: https://www.graphpad.com/guides/prism/7/statistics/index.htm?stat_the_lognormal_distribution.htm.